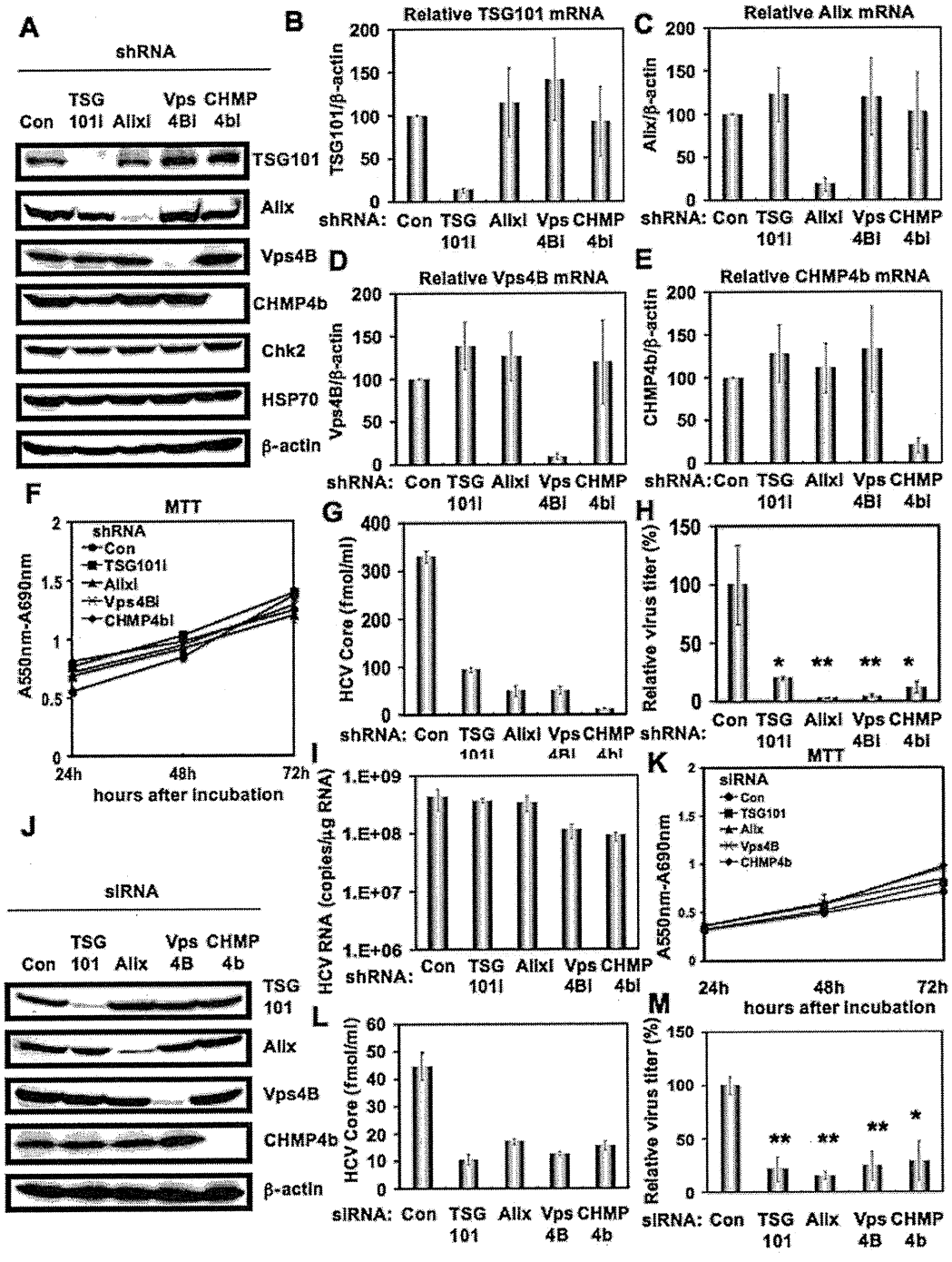

Figure 1. ESCRT components are required for the infectious HCV production. (A) Inhibition of TSG101, Alix, Vps4B, or CHMP4b protein expression by shRNA-producing lentiviral vectors. The results of the Western blot analysis of cellular lysates with anti-TSG101, anti-Alix, anti-Vps4B, anti-CHMP4b, anti-Chk2, anti-HSP70, or anti-β-actin antibody in RSc cells expressing shRNA targeted to TSG101 (TSG101i), Alix (Alixi), Vps4B (Vps4Bi), or CHMP4b (CHMP4bi) as well as in RSc cells transduced with a control lentiviral vector (Con) are shown. Real-time LightCycler RT-PCR for TSG101 (B), Alix (C), Vps4B (D), or CHMP4b mRNA (E) was performed as well as for β-actin mRNA in triplicate. Each mRNA level was calculated relative to the level in RSc cells transduced with a control lentiviral vector (Con) which was assigned as 100%. Error bars in this panel and other figures indicate standard deviations. (F) MTT assay of each knockdown RSc cells at the indicated time. (G) The levels of HCV Core in the culture supernatants from the stable knockdown RSc cells 97 h after inoculation of HCV-JFH1 at an MOI of 0.1 were determined by ELISA. Experiments were done in triplicate and columns represent the mean Core protein levels. (H) The infectivity of HCV in the culture supernatants from the stable knockdown RSc cells 97 hrs after inoculation of HCV-JFH1 at an MOI of 0.1 was determined by a focus-forming assay at 48 hrs post-infection. Experiments were done in triplicate and each virus titer was calculated relative to the level in RSc cells transduced with a control lentiviral vector (Con) which was assigned as 100%. Asterisks indicate significant differences compared to the control treatment. *$P<0.05$; **$P<0.01$. (I) The level of intracellular genome-length HCV-JFH1 RNA in the cells at 97 hrs post-infection was monitored by real-time LightCycler RT-PCR. Results

from three independent experiments are shown. (J) Inhibition of TSG101, Alix, Vps4B, or CHMP4b protein expression by 72 hrs after transient transfection of RSc cells with a pool of control siRNA (Con) or a pool of siRNA specific for Alix, Vps4B, or CHMP4b (50 nM). The results of the Western blot analysis of cellular lysates with anti-TSG101, anti-Alix, anti-Vps4B, anti-CHMP4b, or anti-β-actin antibody is shown. (K) MTT assay of each knockdown RSc cells at the indicated time. (L) The levels of HCV Core in the culture supernatants were determined by ELISA 24 hrs after inoculation of HCV-JFH1. RSc cells were transiently transfected with a pool of control siRNA (Con) or a pool of siRNA specific for TSG101, Alix, Vps4B, or CHMP4b (50 nM). At 48 hrs after transfection, the cells were inoculated with HCV-JFH1 at an MOI of 5 and incubated for 2 hrs. Then, culture medium was changed and incubated for 22 hrs. Experiments were done in triplicate and each Core level was calculated relative to the level in the culture supernatants from the control cells and indicated below. (M) The infectivity of HCV in the culture supernatants from the transient knockdown RSc cells 24 hrs after inoculation of HCV-JFH1 at an MOI of 5 was determined by a focus-forming assay at 48 hrs post-infection. Experiments were done in triplicate and each virus titer was calculated relative to the level in RSc cells transfected with a control siRNA (Con) which was assigned as 100%. Asterisks indicate significant differences compared to the control treatment. *$P<0.05$; **$P<0.01$.

doi:10.1371/journal.pone.0014517.g001

was significantly suppressed in these knockdown cells after HCV-JFH1 infection (Fig. 1G). Importantly, the infectivity of HCV in the culture supernatants was also significantly suppressed in these knockdown cells (Fig. 1H), while the RNA replication of HCV-JFH1 was not affected in the TSG101 or Alix knockdown cells and was somewhat decreased in the Vps4B and CHMP4b knockdown cells (Fig. 1I). This suggested that the ESCRT system is associated with infectious HCV production. To further confirm whether or not the ESCRT system is involved in HCV production, we analyzed the single-round HCV replication. For this, we used RSc cells transiently transfected with a pool of siRNAs specific for TSG101, Alix, Vps4B, or CHMP4b as well as a pool of control siRNAs (Con) following HCV infection. In spite of very effective knockdown of each ESCRT component (Fig. 1J), we demonstrated that the siRNAs did not affect the cell viabilities by MTT assay (Fig. 1K). Consistent with our finding using the stable knockdown cells, we observed that the release of HCV Core or the infectivity of HCV into the culture supernatants was significantly suppressed in these transient knockdown cells 24 hrs after HCV-JFH1 infection (Fig. 1L and 1M). Furthermore, we examined the effect of siRNA specific for TSG101, Alix, Vps4B, or CHMP4b in HCV RNA replication using the subgenomic JFH1 replicon, JRN/3-5B, encoding *Renilla* luciferase gene for monitoring the HCV RNA replication in HuH-7-derived OR6cJRN/3-5B cells (Fig. 2A and 2B) or an OR6 assay system, which was developed as a luciferase reporter assay system for monitoring genome-length HCV RNA replication (HCV-O, genotype 1b) in HuH-7-derived OR6 cells (Fig. 2C) [17,18]. The results showed that these siRNAs could not affect HCV RNA replication as well as the levels of intracellular NS5A proteins (Fig. 2A–C). Although we have demonstrated that the ESCRT system is required for production of extracellular infectious HCV particles, it is not clear whether or not these findings are associated with the assembly of intracellular infectious particles. To test this point, infectivity of intracellular infectious particles was analyzed following lysis of HCV-JFH1-infected knockdown cells by repetitive freeze and thaw. Consequently, we did not observe any significant effects of siRNAs on the accumulation of intracellular infectious HCV-JFH1, while the accumulation of extracellular HCV was significantly suppressed in these knockdown cells (Fig. 2D and 2E), indicating that inhibition of the ESCRT system does not block the accumulation of intracellular infectious HCV particles. Furthermore, Western blot analysis of cell lysates demonstrated that the level of intracellular HCV Core and NS5A was not affected in these knockdown cells 72 hrs post-infection (Fig. 2F). Thus, we conclude that the ESCRT system is not required for the assembly of infectious particles but the ESCRT system is required for late step of HCV production.

HCV Core can target into lipid droplets in the ESCRT knockdown cells

Since lipid droplets have been shown to be involved in an important cytoplasmic organelle for HCV production [4], we performed immunofluorescence and confocal microscopic analyses to determine whether or not HCV Core misses localization into lipid droplets in the ESCRT knockdown cells. We found that the Core was targeted into lipid droplets even in TSG101 knockdown, Alix knockdown, Vps4B knockdown, or CHMP4b knockdown RSc cells as well as in the control RSc cells after HCV infection (Fig. 3). This suggests that the ESCRT system plays a role in the late step after the Core is targeted into lipid droplets in the HCV life cycle.

HCV Core interacts with CHMP4b

To determine whether or not HCV Core can interact with ESCRT component(s), we examined their subcellular localization by confocal laser scanning microscopy. Consequently, the Core mostly colocalized with CHMP4b-green fluorescent protein (GFP) or FLAG-tagged CHMP4b in the perinuclear region of 293FT cells coexpressing them (Fig. 4A and 4B), while the CHMP4b-GFP alone was slightly diffused in the cytoplasm (Fig. 4A), indicating the recruitment of CHMP4b in the Core-expressing area. Importantly, we observed similar partial colocalization in HCV-JFH1-infected RSc cells expressing CHMP4b-GFP (Fig. 4C), whereas the CHMP4b-GFP alone was diffused in the cytoplasm in the uninfected RSc cells (Fig. 4C), suggesting the interaction of HCV Core with CHMP4b. Unfortunately, we failed to observe endogenous CHMP4b using several commercially available anti-CHMP4b antibody (data not shown). Consistent with a previous report that interaction between HCV Core and NS5A is critical for HCV production [3], we found the partial colocalization of NS5A with CHMP4b-GFP as well as the colocalization of Core with CHMP4b-GFP in HCV-JFH1-infected RSc cells (Fig. 4C). Then, we examined whether or not HCV Core can bind to CHMP4b by immunoprecipitation analysis. 293FT cells transfected with 4 mg of pCHMP4b-GFP, pEGFP C3 (Clontech), pcDNA3-FLAG [19], pcDNA3-FLAG-Alix or pFLAG-CHMP4b and RSc cells 5 days after inoculation of HCV-JFH1 at an MOI of 4 were lysed and performed immunoprecipitation of lysate mixtures of HCV-JFH1-infected RSc cells and 293FT cells expressing CHMP4b-GFP, GFP alone, FLAG-CHMP4b or FLAG-epitope alone with anti-FLAG or anti-GFP antibody. Consequently, we observed that the Core but not the NS5A could bind to FLAG-CHMP4b (Fig. 4D). However, the Core was not immunoprecipitated with anti-FLAG antibody using the lysate mixtures of HCV-JFH1-infected RSc cell lysates and 293FT cells expressing FLAG-epitope alone or FLAG-Alix (Fig. 4D). Furthermore, the Core was coimmunoprecipitated with CHMP4b-GFP but not GFP when lysate mixtures of HCV-JFH1-infected RSc cells and 293FT cells expressing CHMP4b-GFP or GFP alone were used (Fig. 4D). In contrast, we failed to observe the marked colocalization of HCV-JFH1 Core with Myc-tagged TSG101 in HCV-JFH1-infected RSc cells expressing Myc-TSG101 or endogenous Alix in HCV-JFH1-infected RSc cells (Fig. 5A). Thus, we concluded that the HCV Core was associated with CHMP4b.

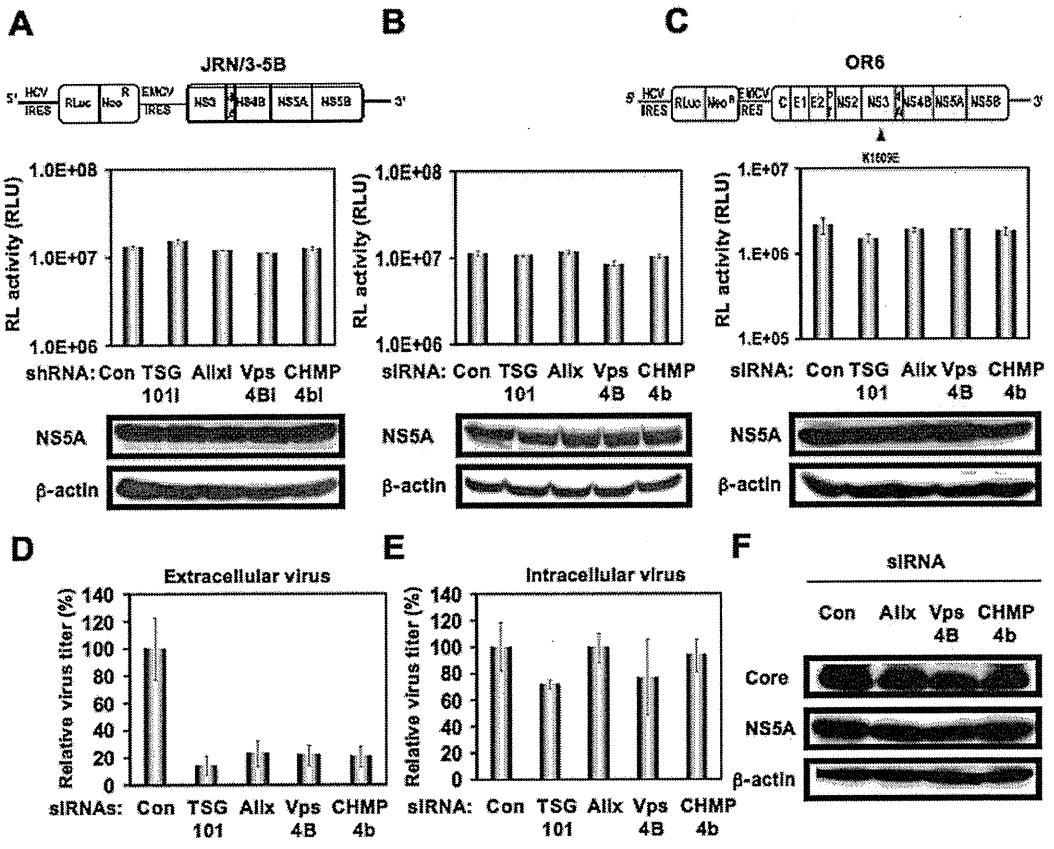

Figure 2. ESCRT system is not required for HCV RNA replication and assembly of intracellular infectious HCV. (A) Schematic gene organization of subgenomic JFH1 (JRN/3-5B) RNA encoding *Renilla* luciferase gene. Renilla luciferase gene (RLuc) is depicted as a box and is expressed as a fusion protein with Neo. The HCV RNA replication level in each ESCRT knockdown OR6c JRN/3-5B cells by lentiviral vector-mediated RNA interference (shRNA) was monitored by RL assay. The RL activity (RLU) is shown. The results shown are means from three independent experiments. (B) 72 hrs after the transfection of OR6c JRN/3-5B polyclonal cells with each of the siRNA (50 nM), the HCV RNA replication level was monitored by RL assay as described in (A). (C) Schematic gene organization of genome-length HCV-O RNA encoding *Renilla* luciferase gene. The position of an adaptive mutation, K1609E, is indicated by a triangle. 72 hrs after the transfection of OR6 cells with each of the siRNA (50 nM), the HCV RNA replication level was monitored by RL assay as described in (A). (D) The infectivity of HCV in the culture supernatants from the transient knockdown RSc cells 24 hrs after inoculation of HCV-JFH1 at an MOI of 2 was determined by a focus-forming assay at 48 hrs post-infection. Experiments were done in triplicate and each virus titer was calculated relative to the level in RSc cells transfected with a control siRNA (Con) which was assigned as 100%. (E) Intracellular HCV infectivity was determined by a focus-forming assay at 48 hrs post-inoculation of lysates by repeated freeze and thaw cycles as described in (D). (F) RSc cells were transiently transfected with a pool of control siRNA (Con) or a pool of siRNA specific for Alix, Vps4B, or CHMP4b (50 nM). At 24 hrs after the transfection, the cells were inoculated with HCV-JFH1 at an MOI of 0.2 and incubated for 48 hrs. Then, culture medium was changed and incubated for 24 hours. Western blotting of cell lysates 72 hrs post-infection with anti-β-actin, anti-HCV NS5A, or anti-HCV Core antibody is shown.
doi:10.1371/journal.pone.0014517.g002

Finally, we examined the subcellular localization of HCV Core and Brox, a novel farnesylated Brol domain-containing protein, since Brox was recently identified as a CHMP4-binding protein [27]. In this context, the Core partially colocalized with GFP-Brox in 293FT cells coexpressing of HCV Core and GFP-Brox (Fig. 5B). Importantly, we observed similar partial colocalization in HCV-JFH1-infected RSc cells expressing GFP-Brox (Fig. 5C). On the other hand, the CHMP4b-GFP alone was diffused in the cytoplasm of uninfected RSc cells (Fig. 5C). To examine the potential role of Brox in HCV life cycle, we established the Brox knockdown RSc cells by lentiviral vector expressing shRNA targeted to Brox (Fig. 5D). Consequently, we found that the release of HCV Core or the infectivity of HCV into the culture supernatants was significantly suppressed in the Brox knockdown cells 4 days after HCV-JFH1 infection (Fig. 5E and 5F), while the RNA replication of HCV-JFH1 was marginally affected in the knockdown cells (Fig. 5G) in spite of the very effective knockdown of Brox mRNA (Fig. 5D), suggesting that Brox is also required for the infectious HCV production.

Discussion

In this study, we have demonstrated that the ESCRT system is required for infectious HCV production, and that HCV Core but not NS5A binds to CHMP4b, a component of ESCRT-III. Although RNA replication of HCV-JFH1 was not affected in the TSG101 knockdown or the Alix knockdown cells, the infectivity of HCV in the culture supernatants was significantly suppressed in these knockdown cells after HCV-JFH1 infection (Fig. 1G and 1H). Furthermore, siRNA targeted to TSG101, Alix, Vps4B, or CHMP4b significantly suppressed HCV Core level or the infectivity of HCV in the culture supernatants (Fig. 1L, 1M, and

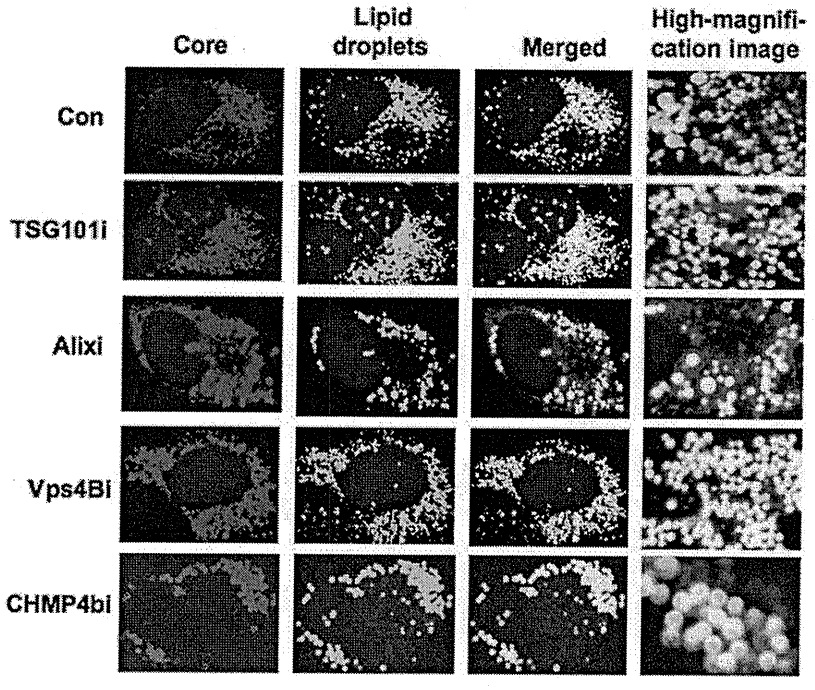

Figure 3. HCV Core is targeted to lipid droplets even in the ESCRT knockdown cells. The RSc cells transduced with a control lentiviral vector (Con), the TSG101 knockdown (TSG101i), the Alix knockdown (Alixi), the Vps4B knockdown (Vps4Bi), or the CHMP4b knockdown (CHMP4bi) cells were infected with HCV-JFH1. Cells were fixed 60 hrs post-infection and were then examined by confocal laser scanning microscopy. Cells were stained with anti-HCV Core (CP-9 and CP-11 mixture) and were then visualized with Cy3 (red). Lipid droplets and nuclei were stained with BODIPY 493/503 (green) and DAPI (blue), respectively. Images were visualized using confocal laser scanning microscopy. Colocalization is shown in yellow (Merged).
doi:10.1371/journal.pone.0014517.g003

2D), while the siRNA did not affect intracellular HCV Core level (Fig. 2E and 2F). Accordingly, we noticed some discrepancy that shRNA targeted to Vps4B or CHMP4b somewhat decreased intracellular HCV RNA replication (Fig. 1I), whereas siRNA targeted to TASG101, Alix, Vps4B or CHMP4b did not affect the RNA replication of subgenomic replicon of JFH1 (Fig. 2A and 2B). Furthermore, siRNAs targeted to TSG101, Alix, Vps4B, or CHMP4b did not affect HCV-O (genotype 1b) RNA replication using the OR6 assay system [17,18] (Fig. 2C), indicating that the ESCRT system is unrelated to the HCV RNA replication of genotype 1b. Thus, we suggested that the ESCRT system is not significant for HCV RNA replication. Within the family *Flaviviridae*, NS3 of the Japanese encephalitis virus (JEV) is also known to interact with TSG101 and microtubules, suggesting their potential roles in JEV assembly [28]. Accordingly, HCV NS3 has been involved in HCV particle assembly and infectivity [29,30]. However, whether HCV NS3 or another HCV protein binds to TSG101 remains to be investigated. At least, we did not observe the interaction between HCV NS5A and CHMP4b (Fig. 4D), Alix (Fig. 4D), TSG101, or Vps4B (data not shown).

Efficient enveloped virus release requires *cis*-acting viral late domains (L-domains), including P(T/S)AP, YPXnL (where X is any amino acid), and PPXY amino acid L-domain motif that are found in the structural proteins of other enveloped viruses [10,11]. Unlike the case with these enveloped viruses, we failed to find the three types of conserved viral L-domain motif in the HCV-JFH1 Core (data not shown). Nevertheless, we observed that the Core bound to CHMP4b, whereas NS5A did not (Fig. 4D), suggesting that the Core has a novel motif required for the HCV production. In this regard, Blanchard *et al.* reported that the aspartic acid at position 111 in the Core is crucial for virus assembly [31]. Interestingly, the conversion of the aspartic acid into alanine at amino acid 111 (PTDP to PTAP), which creates the PTAP L-domain motif, enhanced the release of HCV Core in the cell culture medium (a 2.5-fold increase) compared with the wild-type Core [31]. In contrast, Klein *et al.* demonstrated that the D111A mutation in the Core had no effect on HCV capsid assembly [32]. Furthermore, Murray *et al* found that serine 99, a putative phosphorylation site, in the Core was essential for infectious virion production [7]. In any event, the Core motif that is needed for interaction with the ESCRT components remains to be identified.

Ubiquitin modification of viral protein has been implicated in virion egress as well as in protein turnover. Indeed, the ubiquitin/proteasome system is required for the retrovirus budding machinery, since proteasome inhibition interferes with retroviral Gag polyprotein processing, release, and maturation. The ubiquitin modification of the HIV-1 p6 domain of Gag enhances TSG101 binding [12]. In the case of HCV Core, proteasomal degradation of the Core is mediated by two distinct mechanisms [33–36]. E6AP E3 ubiquitin ligase mediates ubiquitylation and degradation of the Core [34]. In contrast, proteasome activator PA28γ (11S regulator γ), an HCV Core-binding protein, is involved in the ubiquitin-independent degradation of the Core and HCV propagation [33,35,36]. However, little is known whether or not the ubiquitin modification of the Core might be involved in HCV egress like other enveloped viruses.

Finally, the identification of the site of viral particle assembly and budding is an intriguing issue. In case of HCV, at present, it is very difficult to visualize the HCV budding site in the infected cells by an electron microscopy. However, recent studies suggested that lipid droplets are an important cytoplasmic organelle for HCV production [4]. In this regard, Shavinskaya *et al.* demonstrated that

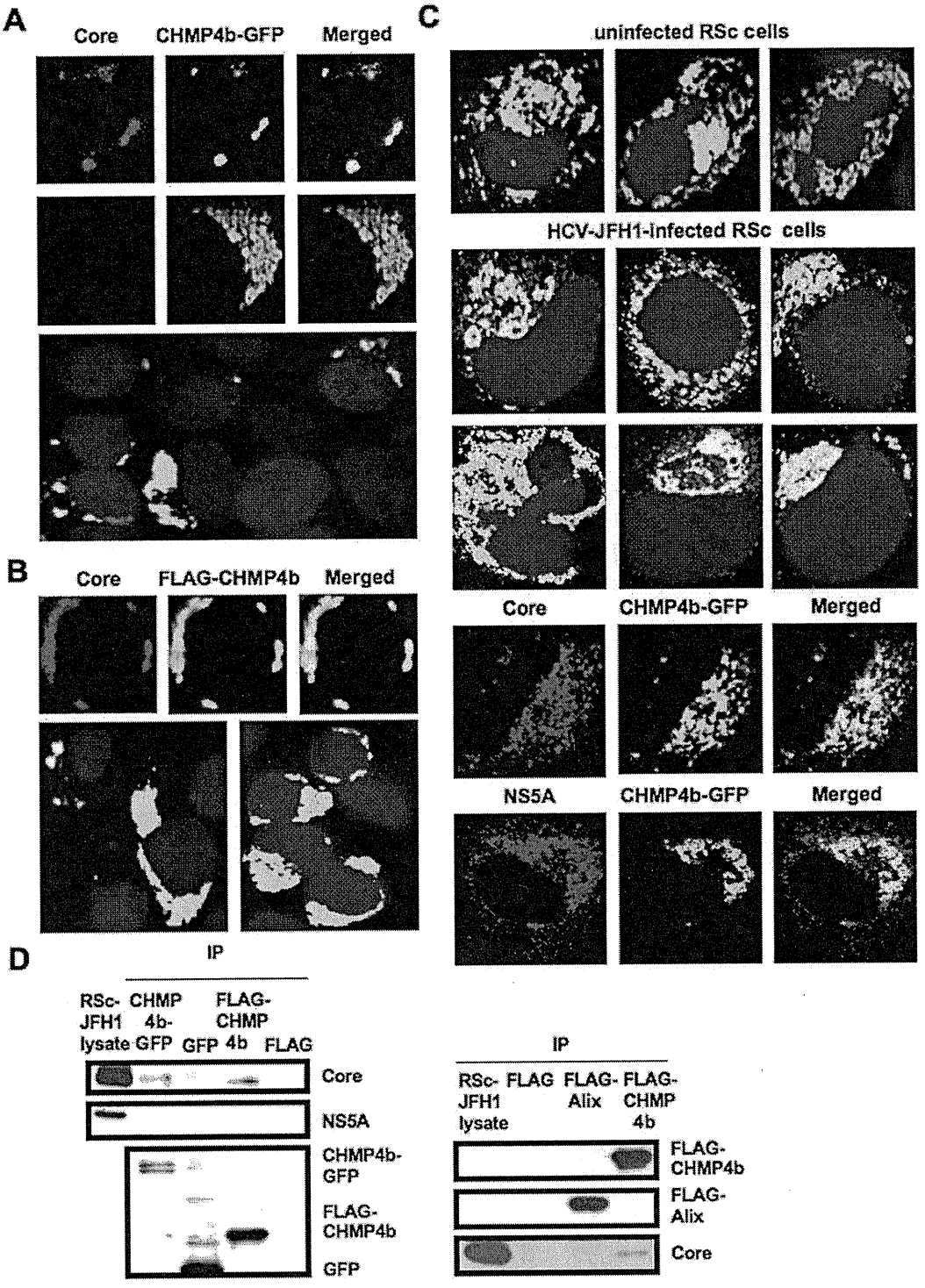

Figure 4. HCV Core interacts with CHMP4b. (A–C) HCV Core colocalizes with CHMP4b. 293FT cells cotransfected with 100 ng of pcDNA3/core (JFH1) and either 100 ng of pCHMP4b-GFP [39] (A) or pFLAG-CHMP4b [39] (B) were examined by confocal laser scanning microscopy. Cells were stained with anti-HCV Core and anti-FLAG polyclonal antibody and were then visualized with FITC (FLAG-CHMP4b) or Cy3 (Core). Images were visualized using confocal laser scanning microscopy. The right panels exhibit the two-color overlay images (Merged). Colocalization is shown in yellow. (C) The Core or NS5A partially colocalizes with CHMP4b in HCV-JFH1-infected RSc cells. RSc cells transfected with 100 ng of pCHMP4b-GFP were infected with HCV-JFH1. Cells were fixed 60 hrs post-infection and were then examined by confocal laser scanning microscopy as shown in panel (A). (D) HCV Core binds to CHMP4b. 293FT cells transfected with 4 μg of pCHMP4b-GFP, pEGFP C3 (Clontech), pcDNA3-FLAG, pcDNA3-FLAG-Alix or pFLAG-CHMP4b and RSc cells 5 days after inoculation of HCV-JFH1 at an MOI of 4 were lysed. The mixtures of these lysates were immunoprecipitated with either anti-FLAG or Living Colors A.v. monoclonal antibody (anti-GFP antibody), followed by immunoblot analysis using anti-HCV Core, anti-HCV NS5A, anti-FLAG, and/or Living Colors A.v. monoclonal antibody.
doi:10.1371/journal.pone.0014517.g004

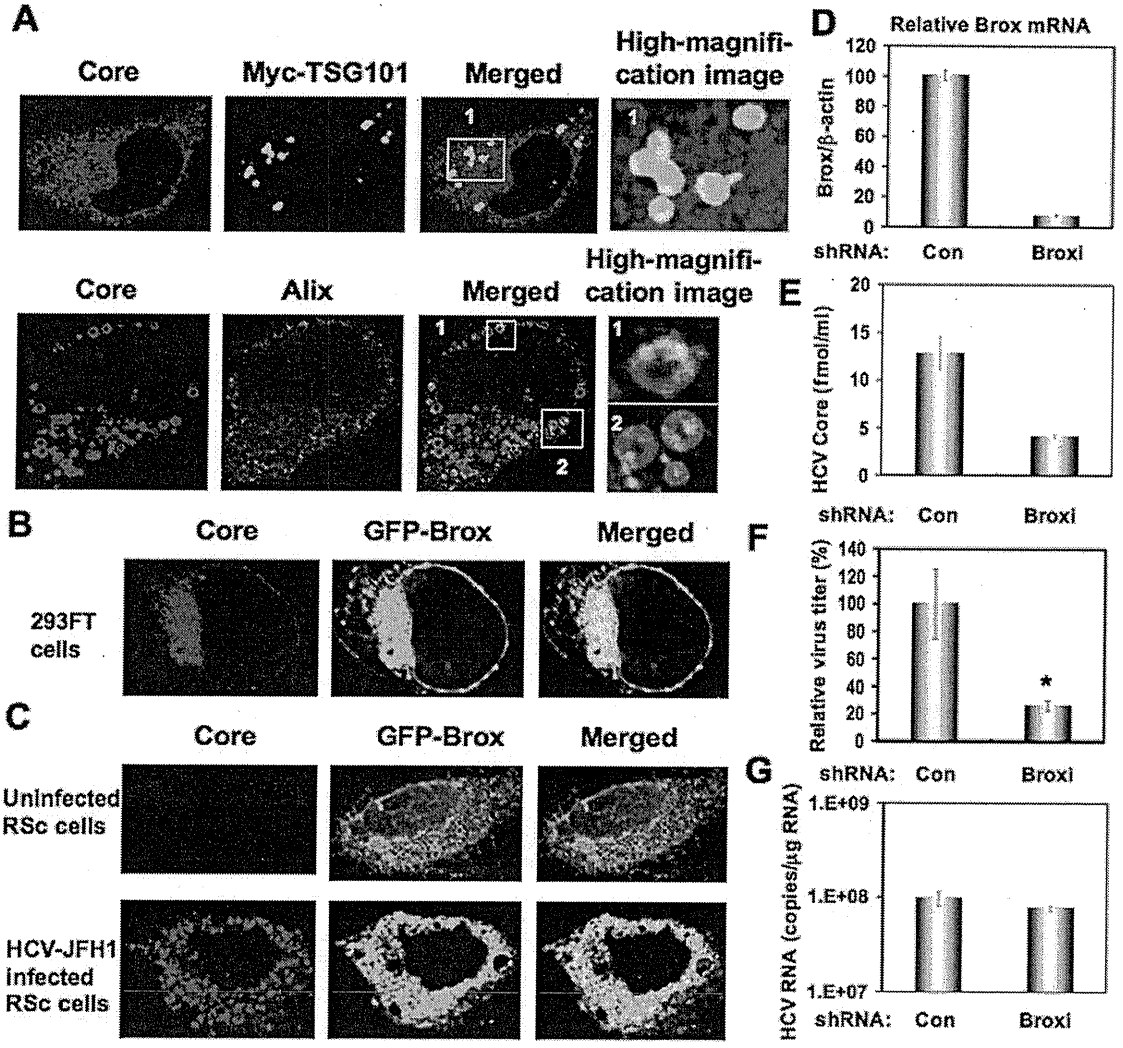

Figure 5. Brox is required for HCV life cycle. (A) Subcellular localization of Myc-tagged TSG101 in HCV-JFH1-infected RSc cells. RSc cells transfected with 100 ng of pBj-Myc-TSG101 [40] were infected with HCV-JFH1. Cells were fixed 60 hrs post-infection and were then examined by confocal laser scanning microscopy as shown in Fig. 3. High magnification image of area 1 is shown. Subcellular localization of endogenous Alix in HCV-JFH1-infected RSc cells 60 hrs post-infection. Cells were stained with anti-Alix and anti-HCV Core antibodies and were examined by confocal laser scanning microscopy. High magnification images of area 1 and area 2 are shown. (B) HCV Core partially colocalizes with Brox. 293FT cells cotransfected with 100 ng of pcDNA3/core (JFH1) and 100 ng of pmGFP-Brox^{WT} [27] were examined by confocal laser scanning microscopy. (C) The HCV Core partially colocalizes with Brox in HCV-JFH1-infected RSc cells. RSc cells transfected with 100 ng of pmGFP-Brox^{WT} were infected with HCV-JFH1. Cells were fixed 60 hrs post-infection and were then examined by confocal laser scanning microscopy. (D) Inhibition of Brox mRNA expression by the shRNA-producing lentiviral vector. Real-time LightCycler RT-PCR for Brox was performed as well as for β-actin mRNA in triplicate. Each mRNA level was calculated relative to the level in RSc cells transduced with a control lentiviral vector (Con) which was assigned as 100%. (E) The levels of HCV Core in the culture supernatants from the Brox knockdown RSc cells (Broxi) 72 hrs after inoculation of HCV-JFH1 were determined by ELISA. (F) The infectivity of HCV in the culture supernatants was determined by a focus-forming assay at 48 hrs post-infection. Experiments were done in triplicate and each virus titer was calculated relative to the level in RSc cells transduced with a control lentiviral vector (Con) which was assigned as 100%. Asterisks indicate significant differences compared to the control treatment. *P<0.05; **P<0.01. (G) The levels of intracellular genome-length HCV-JFH1 RNA in the cells used in (E) were monitored by real-time LightCycler RT-PCR.
doi:10.1371/journal.pone.0014517.g005

the lipid droplet-binding domain of the Core is a major determinant for efficient virus assembly [6]. The HCV Core induces lipid droplet redistribution in a microtubule- and dynein-dependent manner, since disrupting the microtubule network reduced the HCV titer, implicating transport networks in virus assembly and release [2]. Furthermore, Sandrin *et al.* reported that HCV envelope proteins localized to ESCRT-associated multivesicular body (MVB) [37]. Quite recently, Corless *et al.* have demonstrated that Vps4B and the ESCRT-III complex are required for HCV production [38]. Consistent with our findings, their dominant-negative forms of Vps4B and CHMP4B clearly suppressed HCV production. However, their dominant-negative forms of TSG101 and Alix failed to suppress the HCV production and they suggested that both TSG101 and Alix are unrelated to the HCV production. In contrast, we have demonstrated both TSG101 and Alix are also required for the infectious HCV

production by using shRNAs and siRNAs (Fig. 1). We may partly explain such discrepancy due to the difference of the methodology in our study utilized shRNAs and siRNAs instead of dominant-negative forms of TSG101 and Alix. Importantly, they demonstrated that the dominant-negative forms of Vps4B and CHMP4b did not affect the HCV RNA replication and the accumulation of intracellular infectious particles, suggesting that Vps4B and CHMP4b are unrelated to HCV RNA replication. Indeed, we have demonstrated that the ESCRT system is not required for the assembly of intracellular infectious HCV particles (Fig. 2E). Notably, we have demonstrated for the first time that HCV Core associated with CHMP4b (Fig. 4). Accordingly, we have also demonstrated that Brox, a CHMP4b binding protein, is required for HCV production (Fig. 5D–G). Taking together the past and present findings, we propose that the ESCRT system is involved in infectious HCV production after the HCV assembly that occurs on lipid droplets.

Acknowledgments

We thank D. Trono, R. Iggo, R. Agami, A. Takamizawa, and K. Shimotohno for pCMVΔR8.91, pMDG2, pSUPER, pRDI292, and anti-NS5A antibody, respectively. We also thank K. Abe for construction of pJRN/3-5B and T. Nakamura for his technical assistance.

Author Contributions

Conceived and designed the experiments: YA NK. Performed the experiments: YA MK. Analyzed the data: YA. Contributed reagents/materials/analysis tools: MM MI HD TW. Wrote the paper: YA NK.

References

1. Kato N, Hijikata M, Ootsuyama Y, Nakagawa M, Ohkoshi S, et al. (1990) Molecular cloning of the human hepatitis C virus genome from Japanese patients with non-A, non-B hepatitis. Proc Natl Acad Sci USA 87: 9524–9528.
2. Boulant S, Douglas MW, Moody L, Budkowska A, Targett-Adams P, et al. (2008) Hepatitis C virus core protein induces lipid droplet redistribution in a microtubule- and dynein-dependent manner. Traffic 9: 1268–1282.
3. Masaki T, Suzuki R, Murakami K, Aizaki H, Ishii K, et al. (2008) Interaction of hepatitis C virus nonstructural protein 5A with core protein is critical for the production of infectious virus particles. J Virol 82: 7964–7976.
4. Miyanari Y, Atsuzawa K, Usuda N, Watashi K, Hishiki T, et al. (2007) The lipid droplet is an important organelle for hepatitis C virus production. Nat Cell Biol 9: 1089–1097.
5. Shi ST, Polyak SJ, Tu H, Taylor DR, Gretch DR, et al. (2002) Hepatitis C virus NS5A colocalizes with the core protein on lipid droplets and interacts with apolipoproteins. Virology 292: 198–210.
6. Shavinskaya A, Boulant S, Penin F, McLauchlan J, Bartenschlager R (2007) The lipid droplet binding domain of hepatitis C virus core protein is a major determinant for efficient virus assembly. J Biol Chem 282: 37158–37169.
7. Murray CL, Jones CT, Tassello J, Rice CM (2007) Alanine scanning of the hepatitis C virus core protein reveals numerous residues essential for production of infectious virus. J Virol 81: 10220–10231.
8. Appel N, Zayas M, Miller S, Krijnse-Locker J, Schaller T, et al. (2008) Essential role of domain III of nonstructural protein 5A for hepatitis C virus infectious particle assembly. PLOS Pathog 4: e1000035.
9. Tellinghuisen TL, Foss KL, Treadaway J (2008) Regulation of hepatitis C virion production via phosphorylation of the NS5A protein. PLoS Pathog 4: e1000032.
10. Bieniasz PD (2006) Late budding domains and host proteins in enveloped virus release. Virology 344: 55–63.
11. Chen BJ, Lamb RA (2008) Mechanisms for enveloped virus budding: Can some viruses do without an ESCRT? Virology 372: 221–232.
12. Garrus JE, von Schwedler UK, Pornillos OW, Morham SG, Zavitz KH, et al. (2001) Tsg101 and vacuolar protein sorting pathway are essential for HIV-1 budding. Cell 107: 55–65.
13. Wakita T, Pietschmann T, Kato T, Date T, Miyamoto M, et al. (2005) Production of infectious hepatitis C virus in tissue culture from a cloned viral genome. Nat Med 11: 791–796.
14. Ariumi Y, Kuroki M, Abe K, Dansako H, Ikeda M, et al. (2007) DDX3 DEAD-box RNA helicase is required for hepatitis C virus RNA replication. J Virol 81: 13922–13926.
15. Ariumi Y, Kuroki M, Dansako H, Abe K, Ikeda M, et al. (2008) The DNA damage sensors, ataxia-telangiectasia mutated kinase and checkpoint kinase 2 are required for hepatitis C virus RNA replication. J Virol 82: 9639–9646.
16. Kuroki M, Ariumi Y, Ikeda M, Dansako H, Wakita T, et al. (2009) Arsenic trioxide inhibits hepatitis C virus RNA replication through modulation of the glutathione redox system and oxidative stress. J Virol 83: 2338–2348.
17. Ikeda M, Abe K, Dansako H, Nakamura T, Naka K, et al. (2005) Efficient replication of a full-length hepatitis C virus genome, strain O, in cell culture, and development of a luciferase reporter system. Biochem Biophys Res Commun 329: 1350–1359.
18. Ikeda M, Abe K, Yamada M, Dansako H, Naka K, et al. (2006) Different anti-HCV profiles of statins and their potential combination therapy with interferon. Hepatology 44: 117–125.
19. Ariumi Y, Kaida A, Hatanaka M, Shimotohno K (2001) Functional cross-talk of HIV-1 Tat with p53 through its C-terminal domain. Biochem Biophys Res Commun 287: 556–561.
20. Abe K, Ikeda M, Ariumi Y, Dansako H, Wakita T, et al. (2009) HCV genotype 1b chimeric replicon with NS5B of JFH-1 exhibited resistance to cyclosporine A. Arch Virol 154: 1671–1677.
21. Ariumi Y, Ego T, Kaida A, Matsumoto M, Pandolfi PP, et al. (2003) Distinct nuclear body components, PML and SMRT, regulate the trans-acting function of HTLV-1 Tax oncoprotein. Oncogene 22: 1611–1619.
22. Brummelkamp TR, Bernard R, Agami R (2002) A system for stable expression of short interfering RNAs in mammalian cells. Science 296: 550–553.
23. Bridge AJ, Pebernard S, Ducraux A, Nicoulaz AL, Iggo R (2003) Induction of an interferon response by RNAi vectors in mammalian cells. Nat Genet 34: 263–264.
24. Ariumi Y, Priscilla T, Masutani M, Trono D (2005) DNA damage sensors ATM, ATR, DNA-PKcs, and PARP-1 are dispensable for human immunodeficiency virus type 1 integration. J Virol 79: 2973–2978.
25. Naldini L, Blömer U, Gallay P, Ory D, Mulligan R, et al. (1996) In vivo gene delivery and stable transduction of non-dividing cells by a lentiviral vector. Science 272: 263–267.
26. Zufferey R, Nagy D, Mandel RJ, Naldini L, Trono D (1997) Multiply attenuated lentiviral vector achieves efficient gene delivery in vivo. Nat Biotechnol 15: 871–875.
27. Ichioka F, Kobayashi R, Katoh K, Shibata H, Maki M (2008) Brox, a novel farnesylated Bro1 domain-containing protein that associates with charged multivesicular body protein 4 (CHMP4). FEBS J 275: 682–692.
28. Chiou CT, Hu CCA, Chen PH, Liao CL, Lin YL, et al. (2003) Association of Japanese encephalitis virus NS3 protein with microtubules and tumor susceptibility gene 101 (TSG101) protein. J Gen Virol 84: 2795–2805.
29. Yi M, Ma Y, Yates J, Lemon SM (2007) Compensatory mutations in E1, p7, NS2, and NS3 enhance yields of cell culture-infectious intergenotypic chimeric hepatitis C virus. J Virol 81: 629–638.
30. Ma Y, Yates J, Liang Y, Lemon SM, Yi M (2008) NS3 helicase domains involved in infectious intracellular hepatitis C virus particle assembly. J Virol 82: 7624–7639.
31. Blanchard E, Hourioux C, Brand D, Ait-Goughoulte M, Moreau A, et al. (2003) Hepatitis C virus-like particle budding: Role of the core protein and importance of its Asp^{111}. J Virol 77: 10131–10138.
32. Klein KC, Dellos SR, Lingappa JR (2005) Identification of residues in hepatitis C virus core protein that are critical for capsid assembly in a cell-free system. J Virol 79: 6814–6826.
33. Moriishi K, Okabayashi T, Nakai K, Moriya K, Koike K, et al. (2003) Proteasome activator 28γ-dependent nuclear retention and degradation of hepatitis C virus core protein. J Virol 77: 10237–10249.
34. Shirakawa M, Murakami K, Ichimura T, Suzuki R, Shimoji T, et al. (2007) E6AP ubiquitin ligase mediates ubiquitylation and degradation of hepatitis C virus core protein. J Virol 81: 1174–1185.
35. Suzuki R, Moriishi K, Fukuda K, Shirakura M, Ishii K, et al. (2009) Proteasomal turnover of hepatitis C virus core protein is regulated by two distinct mechanisms: a ubiquitin-dependent mechanism and a ubiquitin-independent but PA28γ-dependent mechanism. J Virol 83: 2389–2392.
36. Moriishi K, Shoji I, Mori R, Suzuki R, Suzuki T, et al. (2010) Involvement of PA28gamma in the propagation of hepatitis C virus. Hepatology 52: 411–420.
37. Sandrin V, Boulanger P, Penin F, Granier C, Cosset FL, et al. (2005) Assembly of functional hepatitis C virus glycoproteins on infectious pseudoparticles occurs intracellularly and requires concomitant incorporation of E1 and E2 glycoproteins. J Gen Virol 86: 3189–3199.
38. Corless L, Crump CM, Griffin SD, Harris M (2010) Vps4 and ESCRT-III complex are required for the release of infectious hepatitis C virus particles. J Gen Virol 91: 362–372.
39. Katoh K, Shibata H, Suzuki H, Nara A, Ishidoh K, et al. (2003) The ALG-2-interacting protein Alix associates with CHMP4b, a human homologue of yeast Snf7 that is involved in multivesicular body sorting. J Biol Chem 278: 39104–39113.
40. Katoh K, Suzuki H, Terasawa Y, Mizuno T, Yasuda J, et al. (2005) The penta-EF-hand protein ALG-2 interacts directly with the ESCRT-I component TSG101, and Ca^{2+}-dependently co-localizes to aberrant endosomes with dominant-negative AAA ATPase SKD1/Vps4B. Biochem J 391: 677–685.

JOURNAL OF VIROLOGY, July 2011, p. 6882–6892
0022-538X/11/$12.00 doi:10.1128/JVI.02418-10

Vol. 85, No. 14

Hepatitis C Virus Hijacks P-Body and Stress Granule Components around Lipid Droplets▽

Yasuo Ariumi,[1,2]* Misao Kuroki,[1] Yukihiro Kushima,[3] Kanae Osugi,[4] Makoto Hijikata,[3] Masatoshi Maki,[4] Masanori Ikeda,[1] and Nobuyuki Kato[1]

Department of Tumor Virology, Okayama University Graduate School of Medicine, Dentistry, and Pharmaceutical Sciences, Okayama 700-8558, Japan[1]; Center for AIDS Research, Kumamoto University, Kumamoto 860-0811, Japan[2]; Department of Viral Oncology, Institute for Virus Research, Kyoto University, Kyoto 606-8507, Japan[3]; and Department of Applied Molecular Biosciences, Graduate School of Bioagricultural Sciences, Nagoya University, Nagoya 464-8601, Japan[4]

Received 19 November 2010/Accepted 21 April 2011

The microRNA miR-122 and DDX6/Rck/p54, a microRNA effector, have been implicated in hepatitis C virus (HCV) replication. In this study, we demonstrated for the first time that HCV-JFH1 infection disrupted processing (P)-body formation of the microRNA effectors DDX6, Lsm1, Xrn1, PATL1, and Ago2, but not the decapping enzyme DCP2, and dynamically redistributed these microRNA effectors to the HCV production factory around lipid droplets in HuH-7-derived RSc cells. Notably, HCV-JFH1 infection also redistributed the stress granule components GTPase-activating protein (SH3 domain)-binding protein 1 (G3BP1), ataxin-2 (ATX2), and poly(A)-binding protein 1 (PABP1) to the HCV production factory. In this regard, we found that the P-body formation of DDX6 began to be disrupted at 36 h postinfection. Consistently, G3BP1 transiently formed stress granules at 36 h postinfection. We then observed the ringlike formation of DDX6 or G3BP1 and colocalization with HCV core after 48 h postinfection, suggesting that the disruption of P-body formation and the hijacking of P-body and stress granule components occur at a late step of HCV infection. Furthermore, HCV infection could suppress stress granule formation in response to heat shock or treatment with arsenite. Importantly, we demonstrate that the accumulation of HCV RNA was significantly suppressed in DDX6, Lsm1, ATX2, and PABP1 knockdown cells after the inoculation of HCV-JFH1, suggesting that the P-body and the stress granule components are required for the HCV life cycle. Altogether, HCV seems to hijack the P-body and the stress granule components for HCV replication.

Hepatitis C virus (HCV) is the causative agent of chronic hepatitis, which progresses to liver cirrhosis and hepatocellular carcinoma. HCV is an enveloped virus with a positive single-stranded 9.6-kb RNA genome, which encodes a large polyprotein precursor of approximately 3,000 amino acid (aa) residues. This polyprotein is cleaved by a combination of the host and viral proteases into at least 10 proteins in the following order: core, envelope 1 (E1), E2, p7, nonstructural 2 (NS2), NS3, NS4A, NS4B, NS5A, and NS5B (12, 13, 21). The HCV core protein, a nucleocapsid, is targeted to lipid droplets (LDs), and the dimerization of the core protein by a disulfide bond is essential for the production of infectious virus (24). Recently, LDs have been found to be involved in an important cytoplasmic organelle for HCV production (26). Budding is an essential step in the life cycle of enveloped viruses. The endosomal sorting complex required for transport (ESCRT) system has been involved in such enveloped virus budding machineries, including that of HCV (5).

DEAD-box RNA helicases with ATP-dependent RNA-unwinding activities have been implicated in various RNA metabolic processes, including transcription, translation, RNA splicing, RNA transport, and RNA degradation (32). Previously, DDX3 was identified as an HCV core-interacting protein by yeast two-hybrid screening (25, 29, 43). Indeed, DDX3 is required for HCV RNA replication (3, 31). DDX6 (Rck/p54) is also required for HCV replication (16, 33). DDX6 interacts with an initiation factor, eukaryotic initiation factor 4E (eIF-4E), to repress the translational activity of mRNP (38). Furthermore, DDX6 regulates the activity of the decapping enzymes DCP1 and DCP2 and interacts directly with Argonaute-1 (Ago1) and Ago2 in the microRNA (miRNA)-induced silencing complex (miRISC) and is involved in RNA silencing. DDX6 localizes predominantly in the discrete cytoplasmic foci termed the processing (P) body. Thus, the P body seems to be an aggregate of translationally repressed mRNPs associated with the translation repression and mRNA decay machinery.

In addition to the P body, eukaryotic cells contain another type of RNA granule termed the stress granule (SG) (1, 6, 22, 30). SGs are aggregates of untranslating mRNAs in conjunction with a subset of translation initiation factors (eIF4E, eIF3, eIF4A, eIFG, and poly(A)-binding protein [PABP]), the 40S ribosomal subunits, and several RNA-binding proteins, including PABP, T cell intracellular antigen 1 (TIA-1), TIA-1-related protein (TIAR), and GTPase-activating protein (SH3 domain)-binding protein 1 (G3BP1). SGs regulate mRNA translation and decay as well as proteins involved in various aspects of mRNA metabolisms. SGs are cytoplasmic phase-dense structures that occur in eukaryotic cells exposed to various environmental stress, including heat, arsenite, viral infection, oxidative conditions, UV irradiation, and hypoxia. Impor-

* Corresponding author. Mailing address: Center for AIDS Research, Kumamoto University, 2-2-1 Honjo, Kumamoto 860-0811, Japan. Phone and fax: 81 96 373 6834. E-mail: ariumi@kumamoto-u.ac.jp.
▽ Published ahead of print on 4 May 2011.

tantly, several viruses target SGs and stress granule components for viral replication (10, 11, 34, 39). Recent studies suggest that SGs and the P body physically interact and that mRNAs may move between the two compartments (1, 6, 22, 28, 30).

miRNAs are a class of small noncoding RNA molecules ~21 to 22 nucleotides (nt) in length. miRNAs usually interact with 3′-untranslated regions (UTRs) of target mRNAs, leading to the downregulation of mRNA expression. Notably, the liver-specific and abundant miR-122 interacts with the 5′-UTR of the HCV RNA genome and facilitates HCV replication (15, 17, 19, 20, 31). Ago2 is at least required for the efficient miR-122 regulation of HCV RNA accumulation and translation (40). However, the molecular mechanism(s) for how DDX6 and miR-122 as well as DDX3 positively regulate HCV replication is not fully understood. Therefore, we investigated the potential role of P-body and stress granule components in HCV replication.

MATERIALS AND METHODS

Cell culture. 293FT cells were cultured in Dulbecco's modified Eagle's medium (DMEM; Invitrogen, Carlsbad, CA) supplemented with 10% fetal bovine serum (FBS). HuH-7-derived RSc cured cells, in which cell culture-generated HCV-JFH1 (JFH1 strain of genotype 2a) (37) could infect and effectively replicate, were cultured in DMEM with 10% FBS as described previously (3–5, 23).

Plasmid construction. To construct pcDNA3-FLAG-DDX6, a DNA fragment encoding DDX6 was amplified from total RNAs derived from RSc cells by reverse transcription (RT)-PCR using KOD-Plus DNA polymerase (Toyobo) and the following pairs of primers: 5′-CGGGATCCAAGATGAGCACGGCC AGAACAGAGAACCCTGTT-3′ (forward) and 5′-CCGCTCGAGTTAAGGT TTCTCATCTTCTACAGGCTCGCT-3′ (reverse). The obtained DNA fragments were subcloned into either BamHI-XhoI site of the pcDNA3-FLAG vector (2), and the nucleotide sequences were determined by BigDye termination cycle sequencing using an ABI Prism 310 genetic analyzer (Applied Biosystems, Foster City, CA).

RNA interference. The following small interfering RNAs (siRNAs) were used: human ATXN2/ATX2/ataxin-2 (siGENOME SMRT pool M-011772-01-005), human PABP1/PABPC1 (siGENOME SMRT pool M-019598-01-005), human Lsm1 (siGENOME SMRT pool M-005124-01-005), human Xrn1 (siGENOME SMRT pool M-013754-01-005), human G3BP1 (ON-TARGETplus SMRT pool L-012099-00-005), human PATL1 (siGENOME SMRT pool M-015591-00-005), and siGENOME nontargeting siRNA pool 1 (D-001206-13-05) (Dharmacon, Thermo Fisher Scientific, Waltham, MA), as a control. siRNAs (25 nM final concentration) were transiently transfected into RSc cells (3–5, 23) using Oligofectamine (Invitrogen) according to the manufacturer's instructions. Oligonucleotides with the following sense and antisense sequences were used for the cloning of short hairpin RNA (shRNA)-encoding sequences targeted to DDX6 (DDX6i) as well as the control nontargeting shRNA (shCon) in a lentiviral vector: 5′-GATCC CCGGAGGAACTAACTCTGAAGTTCAAGAGACTTCAGAGTTAGTTCCT CCTTTTTGGAAA-3′ (sense) and 5′-AGCTTTTCCAAAAAGGAGGAACTAA CTCTGAAGTCTCTTGAACTTCAGAGTTAGTTCCTCCGGG-3′ (antisense) for DDX6i and 5′-GATCCCCGAATCCAGAGGTAATCTACTTCAAGAGA GTAGATTACCTCTGGATTCTTTTTGGAAA-3′ (sense) and 5′-AGCTTTTC CAAAAAGAATCCAGAGGTAATCTACTCTCTTGAAGTAGATTACCTC TGGATTCGGG-3′ (antisense) for shCon. The oligonucleotides described above were annealed and subcloned into the BglII-HindIII site, downstream from an RNA polymerase III promoter of pSUPER (8), to generate pSUPER-DDX6i and pSUPER-shCon, respectively. To construct pLV-DDX6i and pLV-shCon, the BamHI-SalI fragments of the corresponding pSUPER plasmids were subcloned into the BamHI-SalI site of pRDI292, an HIV-1-derived self-inactivating lentiviral vector containing a puromycin resistance marker allowing for the selection of transduced cells (7). pLV-DDX3i, described previously (3), was used.

Lentiviral vector production. The vesicular stomatitis virus G protein (VSV-G)-pseudotyped HIV-1-based vector system was described previously (27, 44). The lentiviral vector particles were produced by the transient transfection of the second-generation packaging construct pCMV-ΔR8.91 (27, 44), the VSV-G-envelope-expressing plasmid pMDG2, as well as pRDI292 into 293FT cells with FuGene6 reagent (Roche Diagnostics, Mannheim, Germany).

HCV infection experiments. The supernatants were collected from cell culture-generated HCV-JFH1 (37)-infected RSc cells (3–5, 23) at 5 days postinfection and stored at −80°C after filtering through a 0.45-μm filter (Kurabo, Osaka, Japan) until use. For infection experiments with HCV-JFH1, RSc cells (1×10^5 cells/well) were plated onto 6-well plates and cultured for 24 h. We then infected the cells at a multiplicity of infection (MOI) of 1 or 4. The culture supernatants were collected at 24 h postinfection, and the levels of the core protein were determined by an enzyme-linked immunosorbent assay (ELISA) (Mitsubishi Kagaku Bio-Clinical Laboratories, Tokyo, Japan). Total RNA was also isolated from the infected cellular lysates by using an RNeasy minikit (Qiagen, Hilden, Germany) for analysis of intracellular HCV RNA. The infectivity of HCV-JFH1 in the culture supernatants was determined by a focus-forming assay at 48 h postinfection. HCV-JFH1-infected cells were detected by using anti-HCV core (CP-9 and CP-11 mixture).

Quantitative RT-PCR analysis. The quantitative RT-PCR analysis of HCV RNA was performed by real-time LightCycler PCR (Roche) as described previously (3–5, 14, 23). We used the following forward and reverse primer sets for the real-time LightCycler PCR: 5′-ATGAGTCATGTGGCAGTGGA-3′ (forward) and 5′-GCTGGCTGTACTTCCTCCAC-3′ (reverse) for DDX3, 5′-ATG AGCACGGCCAGAACAGA-3′ (forward) and 5′-TTGCTGTGTCTGTGTGC CCC-3′ (reverse) for DDX6, 5′-TGACGGGGTCACCCACACTG-3′ (forward) and 5′-AAGCTGTAGCCGCGCTCGGT-3′ (reverse) for β-actin, and 5′-AGA GCCATAGTGGTCTGCGG-3′ (forward) and 5′-CTTTCGCAACCCAACGC TAC-3′ (reverse) for HCV-JFH1.

Preparation of anti-PATL1 antibody. The anti-PATL1 antiserum was raised in rabbits using the glutathione *S*-transferase (GST)-fused PATL1 Ct (C-terminal region of PATL1, aa 450 to 770) as an antigen, and immunoglobulins were affinity purified by using the maltose-binding protein (MBP)-fused PATL1 Ct that was immobilized on an *N*-hydroxysuccinimide (NHS) column (GE Healthcare Bio-Sciences AB, Uppsala, Sweden).

Preparation of LDs. Lipid droplets (LDs) were prepared as described previously (26). Cells were pelleted by centrifugation at 1,500 rpm. The pellet was resuspended in hypotonic buffer (50 mM HEPES [pH 7.4], 1 mM EDTA, 2 mM $MgCl_2$) supplemented with a protease inhibitor cocktail (Nacalai Tesque, Kyoto, Japan) and was incubated for 10 min at 4°C. The suspension was homogenized with 30 strokes of a glass Dounce homogenizer using a tight-fitting pestle (Wheaton, Millville, NJ). A 1/10 volume of 10× isotonic buffer {0.2 M HEPES (pH 7.4), 1.2 M potassium acetate (KoAc), 40 mM magnesium acetate [$Mg(oAc)_2$], and 50 mM dithiothreitol (DTT)} was added to the homogenate. The nuclei were removed by centrifugation at 2,000 rpm for 10 min at 4°C. The supernatant was collected and centrifuged at 16,000 × *g* for 10 min at 4°C. The supernatant was mixed with an equal volume of 1.04 M sucrose in isotonic buffer (50 mM HEPES, 100 mM KCl, 2 mM $MgCl_2$, and protease inhibitor cocktail). The solution was set in a 13.2-ml Polyallomer centrifuge tube (Beckman Coulter, Brea, CA). One milliliter of isotonic buffer was loaded onto the sucrose mixture. The tube was centrifuged at 100,000 × *g* in an SW41Ti rotor (Beckman Coulter) for 1 h at 4°C. After the centrifugation, the LD fraction on the top of the gradient solution was recovered in phosphate-buffered saline (PBS). The collected LD fraction was used for Western blot analysis.

Western blot analysis. Cells were lysed in a buffer containing 50 mM Tris-HCl (pH 8.0), 150 mM NaCl, 4 mM EDTA, 1% Nonidet P-40, 0.1% sodium dodecyl sulfate (SDS), 1 mM DTT, and 1 mM phenylmethylsulfonyl fluoride. Supernatants from these lysates were subjected to SDS-polyacrylamide gel electrophoresis, followed by immunoblot analysis using anti-DDX3 (catalog no. 54257 [NT] and 5428 [IN]; Anaspec, San Jose, CA), anti-DDX6 (A300-460A; Bethyl Laboratories, Montgomery, TX), anti-adipose differentiation-related protein (ADFP; GTX110204; GeneTex, San Antonio, TX), anti-calnexin (NT; Stressgen, Ann Arbor, MI), anti-HCV core (CP-9 and CP-11; Institute of Immunology, Tokyo, Japan), anti-β-actin antibody (A5441; Sigma, St. Louis, MO), anti-ATX2/SCA2 antibody (A302-033A; Bethyl), anti-PABP (sc-32318 [10E10]; Santa Cruz Biotechnology, Santa Cruz, CA), anti-PABP (ab21060; Abcam, Cambridge, United Kingdom), anti-G3BP1 (611126; BD Transduction Laboratories, San Jose, CA), anti-LSM1 (LS-C97364, Life Span Biosciences, Seattle, WA), anti-HSP70 (610607; BD), anti-XRN1 (A300-443A; Bethyl), or anti-PATL1 antibody.

Immunofluorescence and confocal microscopic analysis. Cells were fixed in 3.6% formaldehyde in PBS, permeabilized in 0.1% NP-40 in PBS at room temperature, and incubated with anti-DDX3 antibody (54257 [NT] and 5428 [IN]; Anaspec), anti-DDX3X (LS-C64576; Life Span), anti-DDX6 (A300-460A; Bethyl), anti-HCV core (CP-9 and CP-11), anti-ATX2/SCA2 antibody (A302-033A; Bethyl), anti-ataxin-2 (611378; BD), anti-PABP (ab21060; Abcam), anti-G3BP1 (A302-033A; Bethyl), anti-LSM1 (LS-C97364; Life Span), anti-XRN1

(A300-443A; Bethyl), anti-Dcp2 (A302-597A; Bethyl), anti-human Ago2 (011-22033; Wako, Osaka, Japan), or anti-PATL1 antibody at a 1:300 dilution in PBS containing 3% bovine serum albumin (BSA) for 30 min at 37°C. The cells were then stained with fluorescein isothiocyanate (FITC)-conjugated anti-rabbit antibody (Jackson ImmunoResearch, West Grove, PA) at a 1:300 dilution in PBS containing BSA for 30 min at 37°C. Lipid droplets and nuclei were stained with borondipyrromethene (BODIPY) 493/503 (Molecular Probes, Invitrogen) and DAPI (4′,6-diamidino-2-phenylindole), respectively, for 15 min at room temperature. Following extensive washing in PBS, the cells were mounted onto slides using a mounting medium of 90% glycerin–10% PBS with 0.01% *p*-phenylenediamine added to reduce fading. Samples were viewed under a confocal laser scanning microscope (LSM510; Zeiss, Jena, Germany).

Statistical analysis. A statistical comparison of the infectivities of HCV in the culture supernatants between the knockdown cells and the control cells was performed by using the Student *t* test. *P* values of less than 0.05 were considered statistically significant. All error bars indicate standard deviations.

RESULTS

HCV infection hijacks the P-body components. To investigate the potential role of P-body components in the HCV life cycle, we first examined the alteration of the subcellular localization of DDX3 or DDX6 by HCV-JFH1 infection using confocal laser scanning microscopy as previously described (2), since both DDX3 and DDX6 were identified previously as P-body components (6). For this, we used HuH-7-derived RSc cells, in which cell culture-generated HCV-JFH1 (JFH1 strain of genotype 2a) (37) can infect and effectively replicate (3, 4, 23). HCV-JFH1-infected RSc cells at 60 h postinfection were stained with anti-HCV core antibody, anti-DDX3, and/or anti-DDX6. Lipid droplets (LDs) and nuclei were stained with BODIPY 493/503 and DAPI (4′,6-diamidino-2-phenylindole), respectively. Samples were viewed under a confocal laser scanning microscope. Although we observed that endogenous DDX3 localized in faint cytoplasmic foci in uninfected RSc cells, DDX3 relocalized, formed ringlike structures, and colocalized with the HCV core protein in response to HCV-JFH1 infection (Fig. 1A). On the other hand, endogenous DDX6 was localized in the evident cytoplasmic foci termed P bodies in the uninfected cells (Fig. 1A). DDX6 also relocalized, formed ringlike structures, and colocalized with the core protein in response to HCV-JFH1 infection (Fig. 1A). Although we failed to observe that most of the P bodies of DDX6 perfectly colocalized with DDX3 in uninfected RSc cells (Fig. 1B), we observed a few P bodies of DDX6 colocalized with DDX3 in the uninfected cells (Fig. 1B, arrowheads). Intriguingly, we found that endogenous DDX3 colocalized with endogenous DDX6 in HCV-JFH1-infected cells (Fig. 1B). To further confirm this finding, pHA-DDX3 (41) and pcDNA3-FLAG-DDX6 were cotransfected into 293FT cells. Consequently, we observed that hemagglutinin (HA)-DDX3 colocalized with FLAG-DDX6 in 293FT cells coexpressing HA-DDX3 and FLAG-DDX6 (Fig. 1B), suggesting cross talk of DDX3 with DDX6. Recently, LDs have been found to be involved in an important cytoplasmic organelle for HCV production (26). Indeed, both DDX3 and DDX6 were recruited around LDs in response to HCV infection, while these proteins did not colocalize with LDs in uninfected naïve RSc cells (Fig. 1C). Furthermore, both DDX3 and DDX6 accumulated in the LD fraction of the HCV-JFH1-infected RSc cells; however, we could not detect both proteins in the LD fraction from uninfected control cells (Fig. 1D), suggesting that DDX3 and DDX6 are recruited around LDs in response to HCV infection.

These results suggest that HCV-JFH1 infection disrupts P-body formation. Therefore, we further examined whether or not HCV-JFH1 disrupts the P-body formations of other microRNA effectors, including Ago2; the Sm-like protein Lsm1, which is a subunit of heptameric-ring Lsm1-7, involved in decapping; the 5′-to-3′ exonuclease Xrn1; the decapping activator PATL1; and the decapping enzyme DCP2 (6, 21, 30). As expected, HCV-JFH1 disrupted the P-body formations of Ago2, Lsm1, and Xrn1 as well as PATL1 (Fig. 2). Lsm1, Xrn1, or PATL1 relocalized, formed ringlike structures, and colocalized with the HCV core protein in response to HCV-JFH1 infection, whereas they were localized predominantly in P bodies in uninfected RSc cells (Fig. 2). In fact, we observed that DDX6 colocalized with Ago2, a P-body marker (Fig. 2). In contrast, HCV-JFH1 failed to disrupt the P-body formation of DCP2 (Fig. 2). Thus, these results suggest that HCV disrupts P-body formation through the hijacking of P-body components.

HCV hijacks stress granule components. Since Nonhoff et al. recently reported that DDX6 interacted with ataxin-2 (ATX2) (28), we examined the potential cross talk among DDX6, ATX2, and HCV. Although ATX2 and G3BP1, a well-known stress granule component (36), were dispersed in the cytoplasm at 37°C, both proteins formed discrete aggregates termed stress granules and colocalized with each other in response to heat shock at 43°C for 45 min, indicating that ATX2 is also stress granule component (Fig. 3A). We did not observe prominent colocalization between DDX6 and ATX2 at 37°C (Fig. 3B). In contrast, we found that DDX6 was recruited, juxtaposed, and partially colocalized with stress granules of ATX2 in response to heat shock at 43°C for 45 min in the uninfected RSc cells (Fig. 3B). Notably, ATX2 was recruited, formed the ring-like structures, and partially colocalized with DDX6 in response to HCV-JFH1 infection even at 37°C (Fig. 3B). Furthermore, we noticed that ATX2 was recruited around LDs in HCV-JFH1-infected cells at 72 h postinfection, while ATX2 did not colocalize with LDs in uninfected cells (Fig. 3C), suggesting the colocalization of ATX2 with the HCV core protein in infected cells. Indeed, ATX2 colocalized with the HCV core protein in HCV-JFH1-infected RSc cells at 37°C (Fig. 3D). Moreover, HCV-JFH1 infection induced the colocalization of the core protein with other stress granule components, G3BP1 or PABP1 as well as ATX2 (Fig. 4 and 5). To further confirm our findings, we examined the time course of the redistribution of DDX6 and G3BP1 after inoculation with HCV-JFH1. Consequently, we still detected the P-body formation of DDX6 and dispersed G3BP1 in the cytoplasm, and we did not observe a colocalization between the HCV core protein and DDX6 at 12 and 24 h postinfection (Fig. 4). In contrast, we found that the P-body formation of DDX6 began to be disrupted at 36 h postinfection (Fig. 4). Consistently, G3BP1 formed stress granules at 36 h postinfection (Fig. 4). We then noticed a ringlike formation of DDX6 or G3BP1 and colocalization with the HCV core protein after 48 h postinfection (Fig. 4), suggesting that the disruption of P-body formation and the hijacking of P-body and stress granule components occur in a late step of HCV infection.

We then examined whether or not HCV-JFH1 infection

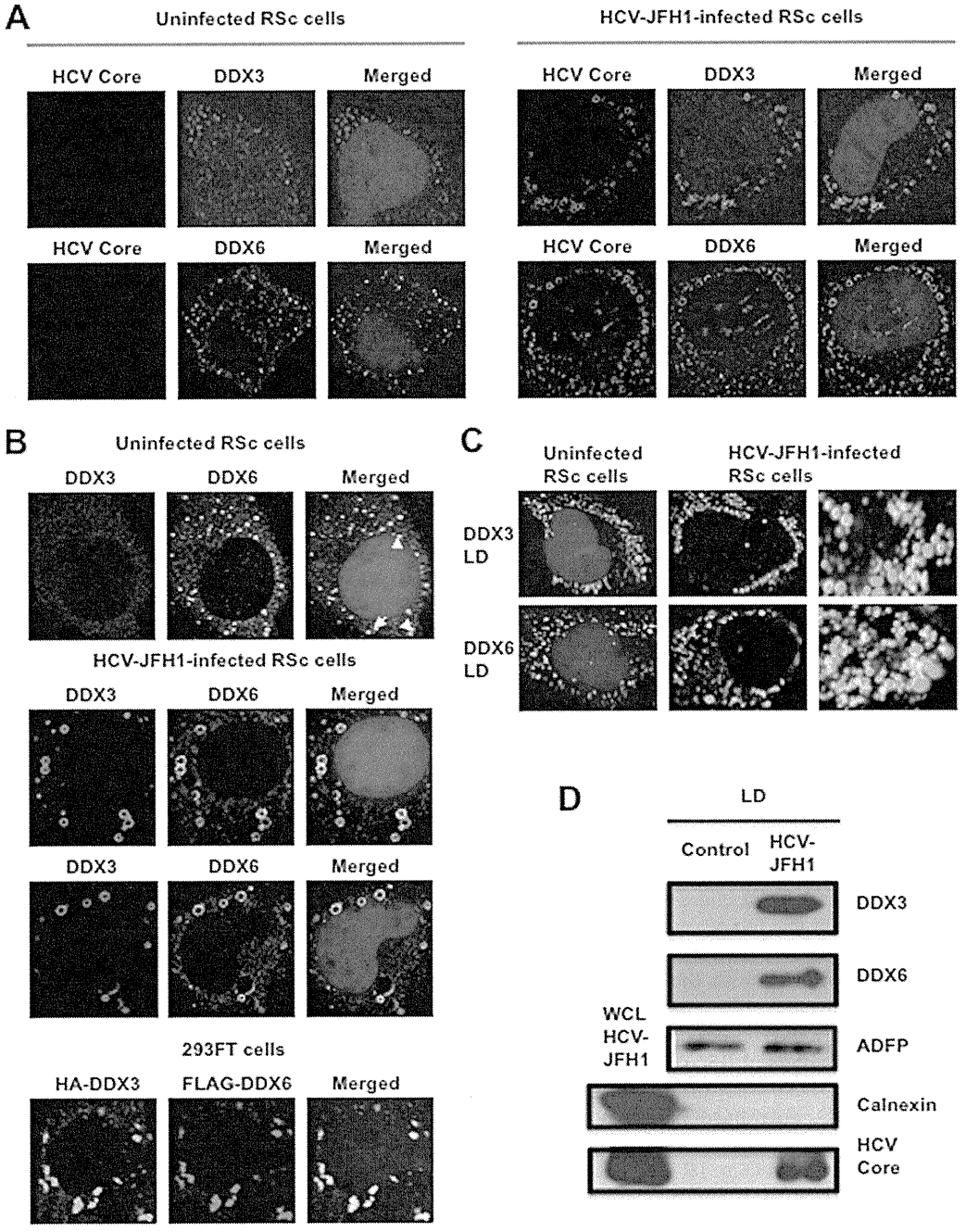

FIG. 1. Dynamic recruitment of DDX3 and DDX6 around lipid droplets (LDs) in response to HCV-JFH1 infection. (A) HCV-JFH1 disrupts the P-body formation of DDX6. Cells were fixed at 60 h postinfection and were then examined by confocal laser scanning microscopy. Cells were stained with anti-HCV core (CP-9 and CP-11 mixture) and either anti-DDX3 (54257 and 54258 mixture) or anti-DDX6 (A300-460A) antibody and then visualized with FITC (DDX3 or DDX6) or Cy3 (core). Images were visualized by using confocal laser scanning microscopy. The two-color overlay images are also exhibited (merged). Colocalization is shown in yellow. (B) HCV-JFH1 recruits DDX3 or DDX6 around LDs. Cells were stained with either anti-DDX3 or anti-DDX6 antibody and were then visualized with Cy3 (red). Lipid droplets and nuclei were stained with BODIPY 493/503 (green) and DAPI (blue), respectively. A high-magnification image is also shown. (C) Colocalization of DDX3 with DDX6. HCV-JFH1-infected RSc cells at 60 h postinfection were stained with anti-DDX3X (LS-C64576) and anti-DDX6 (A300-460A) antibodies. 293FT cells cotransfected with 100 ng of pcDNA3-FLAG-DDX6 and 100 ng of pHA-DDX3 (41) were stained with anti-FLAG-Cy3 and anti-HA-FITC antibodies (Sigma). (D) Association of DDX3 and DDX6 with LDs in response to HCV-JFH1 infection. The LD fraction and whole-cell lysates (WCL) were collected from uninfected RSc cells (control) or HCV-JFH1-infected RSc cells at 5 days postinfection. The results of Western blot analyses of DDX3, DDX6, and the HCV core protein as well as the LD marker ADFP and the endoplasmic reticulum (ER) marker calnexin in the LD fraction are shown.

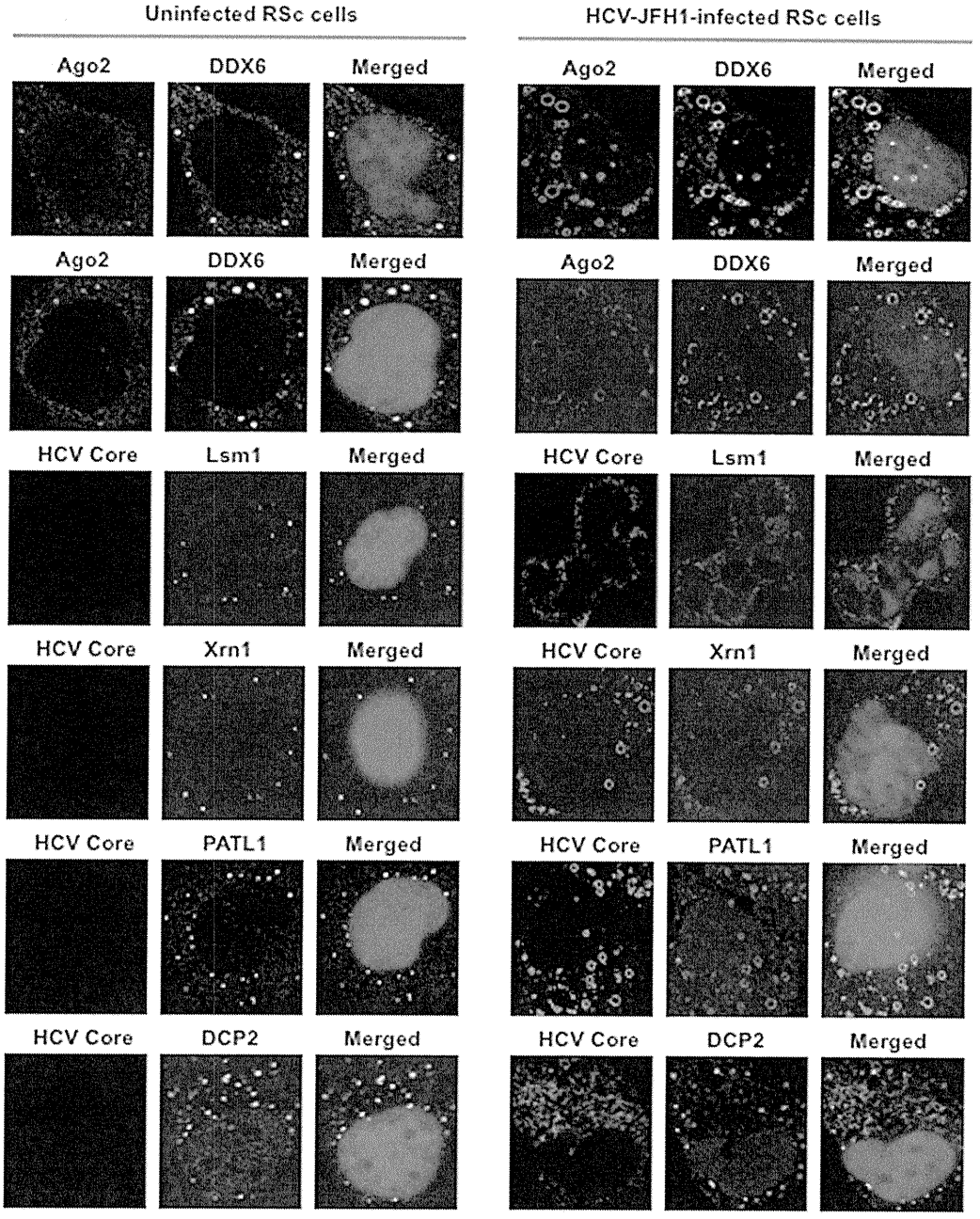

FIG. 2. HCV disrupts the P-body formation of microRNA effectors. Uninfected RSc cells and HCV-JFH1-infected RSc cells at 72 h postinfection were stained with anti-human AGO2 (011-22033) and anti-DDX6 (A300-460A) antibodies. The cells were also stained with anti-HCV core and anti-Lsm1 (LS-C97364), anti-Xrn1 (A300-443A), anti-PATL1, or anti-DCP2 (A302-597A) antibodies and were examined by confocal laser scanning microscopy.

could affect the stress granule formation of G3BP1, ATX2, or PABP1 in response to heat shock or treatment with arsenite. These stress granule components dispersed in the cytoplasm at 37°C, whereas these proteins formed stress granules in response to heat shock at 43°C for 45 min or treatment with 0.5 mM arsenite for 30 min (Fig. 5). In contrast, stress granules were not formed in HCV-JFH1-infected cells at 72 h postinfection in response to heat shock at 43°C for 45 min (Fig. 5), suggesting that HCV-JFH1 infection suppresses stress granule formation in response to heat shock or treatment with arsenite. Intriguingly, G3BP1, ATX2, or PABP1 still colocalized with the HCV core protein even under the above-described stress conditions (Fig. 5). Furthermore, Western blot analysis of cell lysates of uninfected or HCV-JFH1-infected cells at 72 h postinfection showed similar protein expression levels of ATX2, PABP1, HSP70, DDX3, DDX6, and Lsm1 but not G3BP1 (Fig. 6), suggesting that HCV-JFH1 infection does not affect host mRNA translation.

P-body and stress granule components are required for HCV replication. Finally, we investigated the potential role of

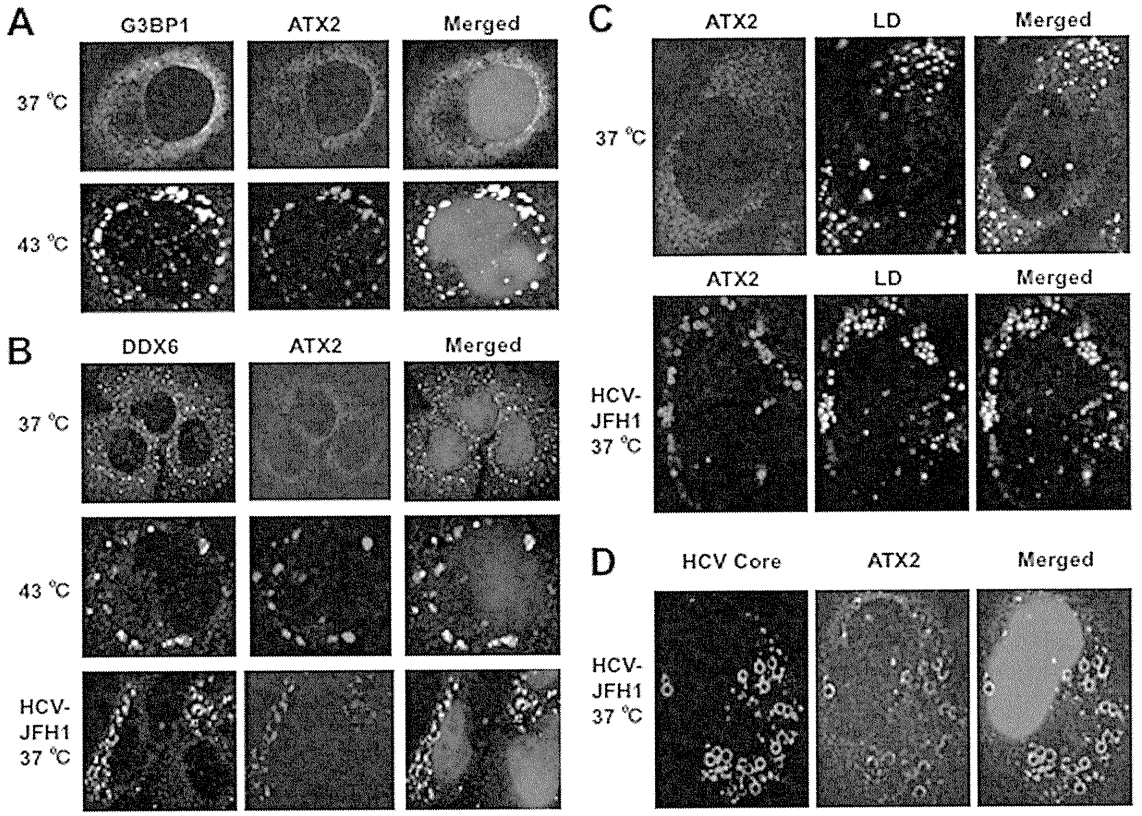

FIG. 3. Dynamic redistribution of ataxin-2 (ATX2) around LDs in response to HCV-JFH1 infection. (A) ATX2 is a stress granule component. RSc cells were incubated at 37°C or 43°C for 45 min. Cells were stained with anti-G3BP1 (A302-033A) and anti-ATX2 (A93520) antibodies and were examined by confocal laser scanning microscopy. (B) Dynamic redistribution of DDX6 and ATX2 in response to heat shock or HCV infection. RSc cells after heat shock at 43°C for 45 min or 72 h after inoculation with HCV-JFH1 were stained with anti-DDX6 and anti-ATX2 (A93520) antibodies. (C) HCV relocalizes ataxin-2 to LDs. HCV-JFH1-infected RSc cells at 72 h postinfection were stained with anti-ATX2 (A93520) antibody and BODIPY 493/503. (D) ATX2 colocalizes with the HCV core protein. HCV-JFH1-infected RSc cells at 72 h postinfection were stained with anti-ATX2/SCA2 (A301-118A) and anti-HCV core antibodies.

P-body and stress granule components in the HCV life cycle. We first used lentiviral vector-mediated RNA interference to stably knock down DDX6 as well as DDX3 in RSc cells. We used puromycin-resistant pooled cells 10 days after lentiviral transduction in all experiments. Real-time LightCycler RT-PCR analysis of DDX3 or DDX6 demonstrated a very effective knockdown of DDX3 or DDX6 in RSc cells transduced with lentiviral vectors expressing the corresponding shRNAs (Fig. 7A). Importantly, shRNAs did not affect cell viabilities (data not shown). We next examined the levels of HCV core and the infectivity of HCV in the culture supernatants as well as the level of intracellular HCV RNA in these knockdown cells 24 h after HCV-JFH1 infection at an MOI of 4. The results showed that the accumulation of HCV RNA was significantly suppressed in DDX3 or DDX6 knockdown cells (Fig. 7B). In this context, the release of the HCV core protein and the infectivity of HCV in the culture supernatants were also significantly suppressed in these knockdown cells (Fig. 7C and D). This finding suggested that DDX6 is required for HCV replication, like DDX3. To further examine the potential role of other P-body and stress granule components in HCV replication, we used RSc cells transiently transfected with a pool of siRNAs specific for ATX2, PABP1, Lsm1, Xrn1, G3BP1, and PATL1 as well as a pool of control siRNAs (siCon) following HCV-JFH1 infection. In spite of the very effective knockdown of each component (Fig. 7E), the siRNAs used in these experiments did not affect cell viabilities (data not shown). Consequently, the accumulation of HCV RNA was significantly suppressed in ATX2, PABP1, or Lsm1 knockdown cells (Fig. 7F), indicting that ATX2, PABP1, and Lsm1 are required for HCV replication. In contrast, the level of HCV RNA was not affected in Xrn1 knockdown cells (Fig. 7F), suggesting that Xrn1 is unrelated to HCV replication. Furthermore, we observed a moderate effect of siG3BP1 and siPATL1 on HCV RNA replication (Fig. 7F). Altogether, HCV seems to hijack the P-body and stress granule components around LDs for HCV replication.

DISCUSSION

So far, the P body and stress granules have been implicated in mRNA translation, RNA silencing, and RNA degradation as well as viral infection (1, 6, 22, 30). Host factors within the P body and stress granules can enhance or limit viral infection, and some viral RNAs and proteins accumulate in the P body and/or stress granules. Indeed, the microRNA effectors DDX6, GW182, Lsm1, and Xrn1 negatively regulate HIV-1 gene expression by preventing the association of viral mRNA

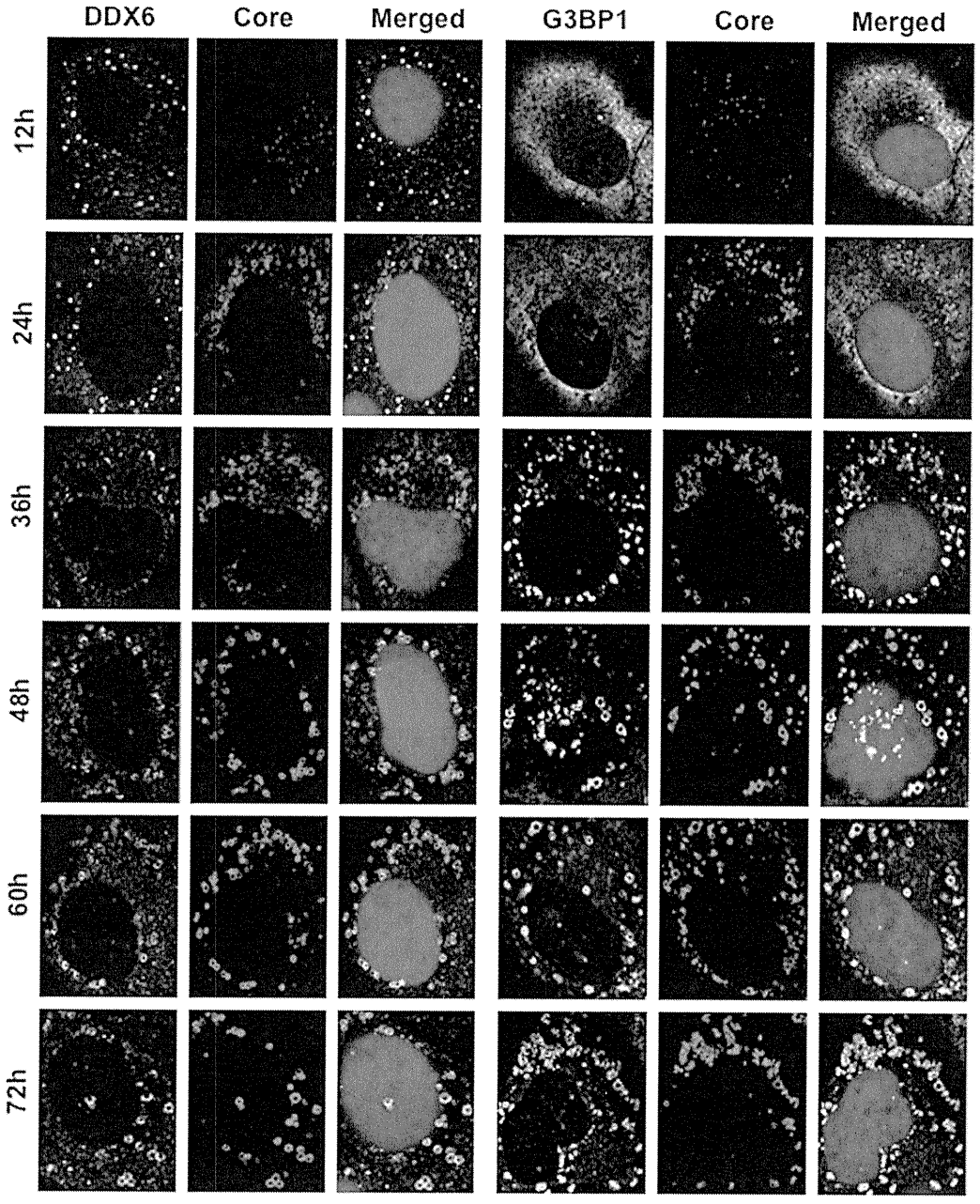

FIG. 4. Dynamic redistribution of DDX6 and G3BP1 in response to HCV-JFH1 infection. RSc cells at the indicated times (hours) after inoculation with HCV-JFH1 were stained with anti-HCV core and either anti-DDX6 (A300-460A) or anti-G3BP1 (A302-033A) antibodies.

with polysomes (9). In contrast, miRNA effectors such as DDX6, Lsm1, PatL1, and Ago2 positively regulate HCV replication (Fig. 7B and F) (16, 31, 33). We have also found that DDX3 and DDX6 are required for HCV RNA replication (3) (Fig. 7B) and that DDX3 colocalized with DDX6 in HCV-JFH1-infected RSc cells (Fig. 1B), suggesting that DDX3 comodulates the DDX6 function in HCV RNA replication. In this regard, the liver-specific miR-122 interacts with the 5′-UTR of the HCV RNA genome and positively regulates HCV replication (15, 17, 19, 20, 31). Since miRNAs usually interact with DDX6 and Ago2 in miRISC and are involved in RNA silencing, DDX6 and Ago2 may be required for miR-122-dependent HCV replication. Indeed, quite recently, a study showed that Ago2 is required for miR-122-dependent HCV RNA replication and translation (40). However, little is known regarding how miR-122 and DDX6 positively regulate HCV replication. Accordingly, we have shown that these miRNA effectors, including DDX6, Lsm1, Xrn1, and Ago2, accumulated around LDs and the HCV production factory and colocalized with the HCV core protein in response to HCV infection (Fig. 1 and 2). However, the decapping enzyme DCP2 did not accumulate and colocalize with the core protein (Fig. 2). Consistent with this finding, Scheller et al. reported previously that the depletion of DCP2 by siRNA did not affect HCV

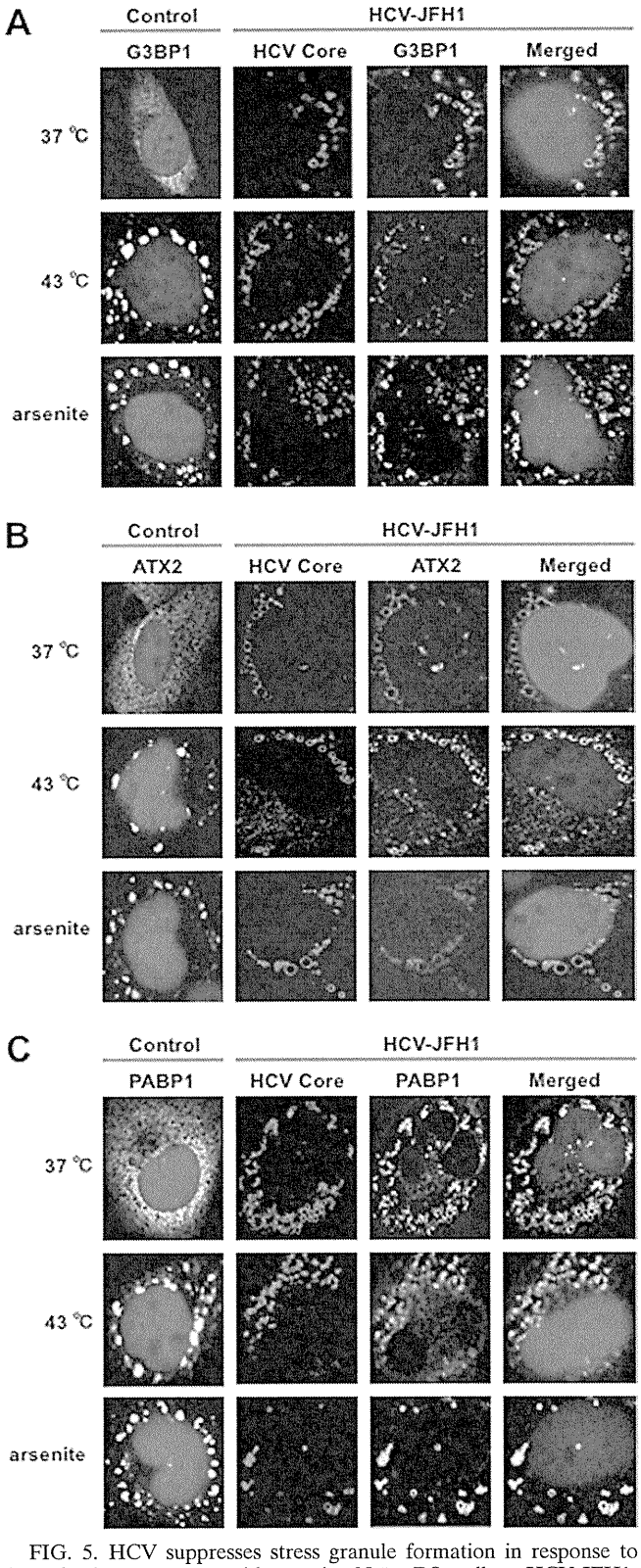

FIG. 5. HCV suppresses stress granule formation in response to heat shock or treatment with arsenite. Naïve RSc cells or HCV-JFH1-infected RSc cells at 72 h postinfection were incubated at 37°C or 43°C for 45 min. Cells were also treated with 0.5 mM arsenite for 30 min. Cells were stained with anti-HCV core and anti-G3BP1 (A), anti-ATX2 (B), or anti-PABP1 (ab21060) (C) antibodies and were examined by confocal laser scanning microscopy.

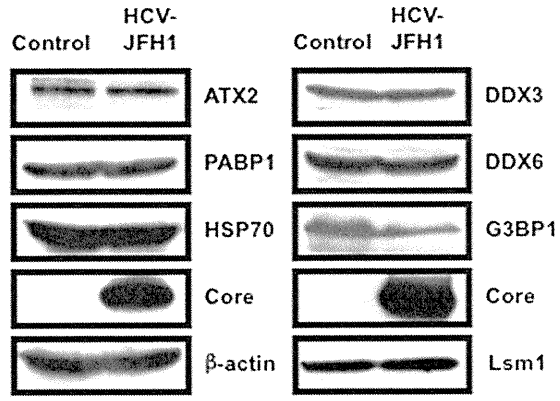

FIG. 6. Host protein expression levels in response to HCV-JFH1 infection. The results of the Western blot analyses of cellular lysates with anti-ATX2/SCA2 antibody (A301-118A), anti-PABP1 (ab21060), anti-HSP70 (610607), anti-HCV core, anti-β-actin, anti-DDX3 (54257 [NT] and 5428 [IN] mixture), anti-DDX6 (A300-460A), anti-G3BP1 (611126), or anti-LSM1 (LS-C97364) antibody in HCV-JFH1-infected RSc cells at 72 h postinfection as well as in naïve RSc cells are shown.

production (33). Since HCV harbors the internal ribosome entry site (IRES) structure in the 5′-UTR of the HCV genome instead of a cap structure, unlike HIV-1, DCP2 may not be recruited on the HCV genome and utilized for HCV replication. Otherwise, DCP2 may determine whether or not DDX6 and miRNAs positively or negatively regulate target mRNA.

Furthermore, we have demonstrated that HCV infection hijacks the P-body and stress granule components around LDs (Fig. 1, 2, 4, and 5). We have found that the P-body formation of DDX6 began to be disrupted at 36 h postinfection (Fig. 4). Consistently, G3BP1 formed stress granules at 36 h postinfection. We then observed the ringlike formation of DDX6 or G3BP1 and colocalization with the HCV core protein after 48 h postinfection, suggesting that the disruption of P-body formation and the hijacking of P-body and stress granule components occur at a late step of HCV infection. Furthermore, HCV infection could suppress stress granule formation in response to heat shock or treatment with arsenite (Fig. 5). In this regard, West Nile virus and dengue virus, of the family *Flaviviridae*, interfere with stress granule formation and P-body assembly through interactions with T cell intracellular antigen 1 (TIA-1)/TIAR (11). Moreover, PABP1 and G3BP1, stress granule components, are known to be common viral targets for the inhibition of host mRNA translation (34, 39). In fact, HIV-1 and poliovirus proteases cleave PABP1 and/or G3BP1 and suppress stress granule formation during viral infection (34, 39). On the other hand, HCV infection transiently induced stress granules at 36 h postinfection (Fig. 4) and did not cleave PABP1 (Fig. 6); however, HCV could suppress stress granule formation in response to heat shock or treatment with arsenite through hijacking their components around LDs, the HCV production factory (Fig. 5). Consistently, Jones et al. showed that HCV transiently induces stress granules of enhanced green fluorescent protein (EGFP)-G3BP at 36 h after infection with the cell culture-generated HCV (HCVcc) reporter virus Jc1FLAG2 (p7-nsGluc2A); however, those authors did not show the recruitment of EGFP-G3BP to LDs (18). Although we do not know the exact reason for this apparent discrepancy,

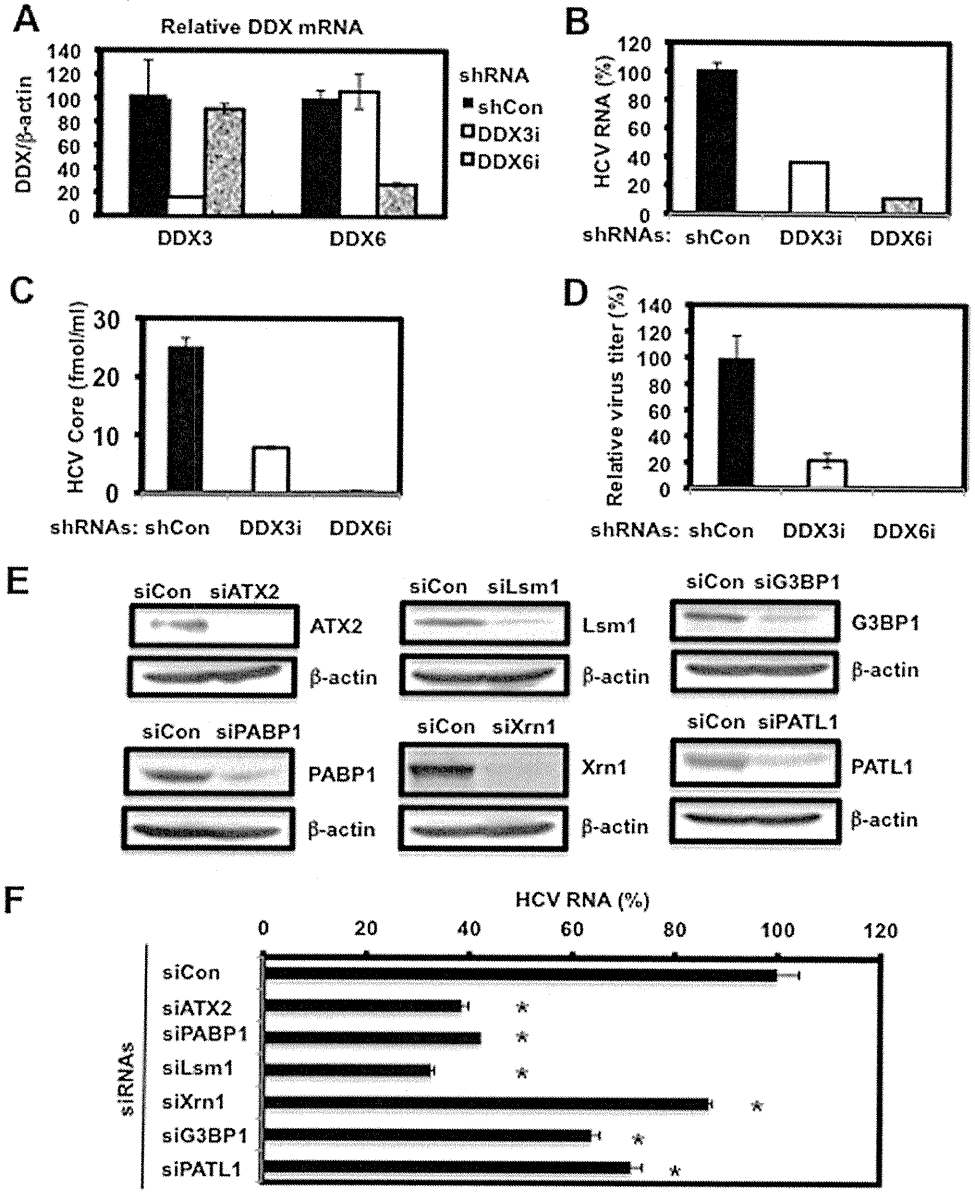

FIG. 7. Requirement of P-body and stress granule components for HCV replication. (A) Inhibition of DDX3 or DDX6 mRNA expression by the shRNA-producing lentiviral vector. Real-time LightCycler RT-PCR for DDX3 or DDX6 was also performed for β-actin mRNA in RSc cells expressing shRNA targeted to DDX3 (DDX3i) or DDX6 (DDX6i) or the control nontargeting shRNA (shCon) in triplicate. Each mRNA level was calculated relative to the level in RSc cells transduced with the control nontargeting lentiviral vector (shCon), which was assigned as 100%. Error bars in this panel and other panels indicate standard deviations. (B) Levels of intracellular genome-length HCV-JFH1 RNA in the cells at 24 h postinfection at an MOI of 4 were monitored by real-time LightCycler RT-PCR. Results from three independent experiments are shown. Each HCV RNA level was calculated relative to the level in RSc cells transduced with a control lentiviral vector (shCon), which was assigned as 100%. (C) The levels of HCV core in the culture supernatants from the stable knockdown RSc cells 24 h after inoculation of HCV-JFH1 at an MOI of 4 were determined by ELISA. Experiments were done in triplicate, and columns represent the mean core protein levels. (D) The infectivity of HCV in the culture supernatants from stable-knockdown RSc cells 24 h after inoculation of HCV-JFH1 at an MOI of 4 was determined by a focus-forming assay at 24 h postinfection. Experiments were done in triplicate, and each virus titer was calculated relative to the level in RSc cells transduced with a control lentiviral vector (shCon), which was assigned as 100%. (E) Inhibition of ATX2, PABP1, Lsm1, Xrn1, G3BP1, or PATL1 protein expression by 72 h after transient transfection of RSc cells with a pool of control nontargeting siRNA (siCon) or a pool of siRNAs specific for ATX2, PABP1, Lsm1, Xrn1, G3BP1, or PATL1 (25 nM), respectively. The results of Western blot analyses of cellular lysates with anti-ATX2, anti-PABP1, anti-Lsm1, anti-Xrn1, anti-G3BP1, anti-PATL1, or anti-β-actin antibody are shown. (F) Levels of intracellular genome-length HCV-JFH1 RNA in the cells at 48 h postinfection at an MOI of 1 were monitored by real-time LightCycler RT-PCR. RSc cells were transiently transfected with a pool of control siRNA (siCon) or a pool of siRNAs specific for ATX2, PABP1, Lsm1, Xrn1, G3BP1, and PATL1 (25 nM). At 48 h after transfection, the cells were inoculated with HCV-JFH1 at an MOI of 1 and incubated for 2 h. The culture medium was then changed and incubated for 22 h. Experiments were done in triplicate, and each HCV RNA level was calculated relative to the level in RSc cells transfected with a control siRNA (siCon), which was assigned as 100%. Asterisks indicate significant differences compared to the control treatment (*, $P <$ 0.01).

several possible explanations can be offered. First, those authors examined the localization of EGFP-G3BP within 48 h postinfection, and we observed it at later times (Fig. 4). Second, they used only EGFP-tagged G3BP instead of endogenous G3BP1. Third, they used a Jc1FLAG2 (p7-nsGluc2A) clone, and an HCV-JFH1 clone could markedly induce the recruitment of the core protein to LDs compared to that of Jc1. Also, Jangra et al. failed to observe the recruitment of DDX6 to LDs at 2 days after infection with HJ3-5 virus (16). Accordingly, we also observed that most of the DDX6 still formed intact P bodies at earlier times (12 h or 24 h postinfection). Importantly, we observed the recruitment of DDX6 to LDs 48 h later (Fig. 4). Furthermore, those authors did not show the ringlike structure formation of the HJ3-5 core protein around LDs, unlike the JFH1 core protein that we used in this study. The interaction of the HCV core protein with DDX6 may explain the recruitment of P-body components to LDs. However, we do not yet know whether the P-body function(s) can be performed on LDs. At least, HCV infection did not affect the translation of several host mRNAs with 5′ caps and 3′ poly(A) tails despite the disruption of P-body formation at 72 h postinfection (Fig. 6), suggesting that HCV does not affect P-body function and that HCV recruits functional P bodies to LDs.

We need to address the potential role of stress granule components, such as PABP1, in HCV replication/translation, since the HCV genome does not harbor the 3′ poly(A) tail. Intriguingly, we have found that the accumulation of HCV RNA was significantly suppressed in PABP1 knockdown RSc cells (Fig. 7F). In this regard, Tingting et al. demonstrated previously that G3BP1 and PABP1 as well as DDX1 were identified as the HCV 3′-UTR RNA-binding proteins by proteomic analysis and that G3BP1 was required for HCV RNA replication (35). Yi et al. also reported that G3BP1 was associated with HCV NS5B and that G3BP1 was required for HCV RNA replication (42). We observed a moderate effect of siG3BP1 on HCV RNA replication (Fig. 7F). In contrast, the accumulation of HCV RNA was significantly suppressed in ATX2 and Lsm1 knockdown cells as well as in PABP1 knockdown cells (Fig. 7F), suggesting that ATX2, Lsm1, and PABP1 are required for HCV replication.

Taking these results together, this study has demonstrated for the first time that HCV hijacks P-body and stress granule components around LDs. This hijacking may regulate HCV RNA replication and translation. Indeed, we have found that the accumulation of genome-length HCV-O (genotype 1b) (14) RNA was markedly suppressed in DDX6 knockdown O cells (data not shown). More importantly, these P-body and stress granule components may be involved in the maintenance of the HCV RNA genome without 5′ cap and 3′ poly(A) tail structures in the cytoplasm for long periods, since the hijacking of P-body and stress granule components by HCV occurred at later times.

ACKNOWLEDGMENTS

We thank D. Trono for the lentiviral vector system, T. Wakita for HCV-JFH1, and K. T. Jeang for pHA-DDX3. We also thank T. Nakamura and K. Takeshita for their technical assistance.

This work was supported by a grant-in-aid for scientific research (C) from the Japan Society for the Promotion of Science (JSPS); by a grant-in-aid for research on hepatitis from the Ministry of Health, Labor, and Welfare of Japan; and by the Viral Hepatitis Research Foundation of Japan. M.K. was supported by a research fellowship from the JSPS for young scientists.

REFERENCES

1. **Anderson, P., and N. Kedersha.** 2007. Stress granules: the Tao of RNA triage. Trends Biochem. Sci. **33**:141–150.
2. **Ariumi, Y., et al.** 2003. Distinct nuclear body components, PML and SMRT, regulate the *trans*-acting function of HTLV-1 Tax oncoprotein. Oncogene **22**:1611–1619.
3. **Ariumi, Y., et al.** 2007. DDX3 DEAD-box RNA helicase is required for hepatitis C virus RNA replication. J. Virol. **81**:13922–13926.
4. **Ariumi, Y., et al.** 2008. The DNA damage sensors ataxia-telangiectasia mutated kinase and checkpoint kinase 2 are required for hepatitis C virus RNA replication. J. Virol. **82**:9639–9646.
5. **Ariumi, Y., et al.** 2011. The ESCRT system is required for hepatitis C virus production. PLoS One **6**:e14517.
6. **Beckham, C. J., and R. Parker.** 2008. P bodies, stress granules, and viral life cycles. Cell Host Microbe **3**:206–212.
7. **Bridge, A. J., S. Pebernard, A. Ducraux, A. L. Nicoulaz, and R. Iggo.** 2003. Induction of an interferon response by RNAi vectors in mammalian cells. Nat. Genet. **34**:263–264.
8. **Brummelkamp, T. R., R. Bernard, and R. Agami.** 2002. A system for stable expression of short interfering RNAs in mammalian cells. Science **296**:550–553.
9. **Chable-Bessia, C., et al.** 2009. Suppression of HIV-1 replication by microRNA effectors. Retrovirology **6**:26.
10. **Cristea, I. M., et al.** 2010. Host factors associated with the Sindbis virus RNA-dependent RNA polymerase: role for G3BP1 and G3BP2 in virus replication. J. Virol. **84**:6720–6732.
11. **Emara, M. M., and M. A. Brinton.** 2007. Interaction of TIA-1/TIAR with West Nile and dengue virus products in infected cells interferes with stress granule formation and processing body assembly. Proc. Natl. Acad. Sci. U. S. A. **104**:9041–9046.
12. **Hijikata, M., N. Kato, Y. Ootsuyama, M. Nakagawa, and K. Shimotohno.** 1991. Gene mapping of the putative structural region of the hepatitis C virus genome by in vitro processing analysis. Proc. Natl. Acad. Sci. U. S. A. **88**:5547–5551.
13. **Hijikata, M., et al.** 1993. Proteolytic processing and membrane association of putative nonstructural proteins of hepatitis C virus. Proc. Natl. Acad. Sci. U. S. A. **90**:10773–10777.
14. **Ikeda, M., et al.** 2005. Efficient replication of a full-length hepatitis C virus genome, strain O, in cell culture, and development of a luciferase reporter system. Biochem. Biophys. Res. Commun. **329**:1350–1359.
15. **Jangra, R. K., M. Yi, and S. M. Lemon.** 2010. Regulation of hepatitis C virus translation and infectious virus production by the microRNA miR-122. J. Virol. **84**:6615–6625.
16. **Jangra, R. K., M. Yi, and S. M. Lemon.** 2010. DDX6 (Rck/p54) is required for efficient hepatitis C virus replication but not IRES-directed translation. J. Virol. **84**:6810–6824.
17. **Ji, H., et al.** 2008. MicroRNA-122 stimulates translation of hepatitis C virus RNA. EMBO J. **27**:3300–3310.
18. **Jones, C. T., et al.** 2010. Real-time imaging of hepatitis C virus infection using a fluorescent cell-based reporter system. Nat. Biotechnol. **28**:167–171.
19. **Jopling, C. L., M. Yi, A. M. Lancaster, S. M. Lemon, and P. Sarnow.** 2005. Modulation of hepatitis C virus RNA abundance by a liver-specific microRNA. Science **309**:1577–1581.
20. **Jopling, C. L., S. Schütz, and P. Sarnow.** 2008. Position-dependent function for a tandem microRNA miR-122-binding site located in the hepatitis C virus RNA genome. Cell Host Microbe **4**:77–85.
21. **Kato, N., et al.** 1990. Molecular cloning of the human hepatitis C virus genome from Japanese patients with non-A, non-B hepatitis. Proc. Natl. Acad. Sci. U. S. A. **87**:9524–9528.
22. **Kedersha, N., and P. Anderson.** 2007. Mammalian stress granules and processing bodies. Methods Enzymol. **431**:61–81.
23. **Kuroki, M., et al.** 2009. Arsenic trioxide inhibits hepatitis C virus RNA replication through modulation of the glutathione redox system and oxidative stress. J. Virol. **83**:2338–2348.
24. **Kushima, Y., T. Wakita, and M. Hijikata.** 2010. A disulfide-bonded dimer of the core protein of hepatitis C virus is important for virus-like particle production. J. Virol. **84**:9118–9127.
25. **Mamiya, N., and H. J. Worman.** 1999. Hepatitis C virus core protein binds to a DEAD box RNA helicase. J. Biol. Chem. **274**:15751–15756.
26. **Miyanari, Y., et al.** 2007. The lipid droplet is an important organelle for hepatitis C virus production. Nat. Cell Biol. **9**:1089–1097.
27. **Naldini, L., et al.** 1996. In vivo gene delivery and stable transduction of nondividing cells by a lentiviral vector. Science **272**:263–267.
28. **Nonhoff, U., et al.** 2007. Ataxin-2 interacts with the DEAD/H-box RNA helicase DDX6 and interferes with P-bodies and stress granules. Mol. Biol. Cell **18**:1385–1396.
29. **Owsianka, A. M., and A. H. Patel.** 1999. Hepatitis C virus core protein interacts with a human DEAD box protein DDX3. Virology **257**:330–340.

30. **Parker, R., and U. Sheth.** 2007. P bodies and the control of mRNA translation and degradation. Mol. Cell **25**:635–646.
31. **Randall, G., et al.** 2007. Cellular cofactors affecting hepatitis C virus infection and replication. Proc. Natl. Acad. Sci. U. S. A. **104**:12884–12889.
32. **Rocak, S., and P. Linder.** 2004. DEAD-box proteins: the driving forces behind RNA metabolism. Nat. Rev. Mol. Cell Biol. **5**:232–241.
33. **Scheller, N., et al.** 2009. Translation and replication of hepatitis C virus genomic RNA depends on ancient cellular proteins that control mRNA fates. Proc. Natl. Acad. Sci. U. S. A. **106**:13517–13522.
34. **Smith, R. W., and N. K. Gray.** 2010. Poly(A)-binding protein (PABP): a common viral target. Biochem. J. **426**:1–11.
35. **Tingting, P., F. Caiyun, Y. Zhigang, Y. Pengyuan, and Y. Zhenghong.** 2006. Subproteomic analysis of the cellular proteins associated with the 3′ untranslated region of the hepatitis C virus genome in human liver cells. Biochem. Biophys. Res. Commun. **347**:683–691.
36. **Tourrière, H., et al.** 2003. The RasGAP-associated endoribonuclease G3BP assembles stress granules. J. Cell Biol. **160**:823–831.
37. **Wakita, T., et al.** 2005. Production of infectious hepatitis C virus in tissue culture from a cloned viral genome. Nat. Med. **11**:791–796.
38. **Weston, A., and J. Sommerville.** 2006. Xp54 and related (DDX6-like) RNA helicase: roles in messenger RNP assembly, translation regulation and RNA degradation. Nucleic Acids Res. **34**:3082–3094.
39. **White, J. P., A. M. Cardenas, W. E. Marissen, and R. E. Lloyd.** 2007. Inhibition of cytoplasmic mRNA stress granule formation by a viral proteinase. Cell Host Microbe **2**:295–305.
40. **Wilson, J. A., C. Zhang, A. Huys, and C. D. Richardson.** 2011. Human Ago2 is required for efficient miR-122 regulation of HCV RNA accumulation and translation. J. Virol. **85**:2342–2350.
41. **Yedavalli, V. S., C. Neuveut, Y. H. Chi, L. Kleiman, and K. T. Jeang.** 2004. Requirement of DDX3 DAED box RNA helicase for HIV-1 Rev-RRE export function. Cell **119**:381–392.
42. **Yi, Z., et al.** 2006. Subproteomic study of hepatitis C virus replicon reveals Ras-GTPase-activating protein binding protein 1 as potential HCV RC component. Biophys. Biochem. Res. Commun. **350**:174–178.
43. **You, L. R., et al.** 1999. Hepatitis C virus core protein interacts with cellular putative RNA helicase. J. Virol. **73**:2841–2853.
44. **Zufferey, R., D. Nagy, R. J. Mandel, L. Naldini, and D. Trono.** 1997. Multiply attenuated lentiviral vector achieves efficient gene delivery in vivo. Nat. Biotechnol. **15**:871–875.

Virus Research 157 (2011) 61–70

Contents lists available at ScienceDirect

Virus Research

journal homepage: www.elsevier.com/locate/virusres

Mechanism of action of ribavirin in a novel hepatitis C virus replication cell system

Kyoko Mori[a], Masanori Ikeda[a], Yasuo Ariumi[a], Hiromichi Dansako[a], Takaji Wakita[b], Nobuyuki Kato[a,*]

[a] Department of Tumor Virology, Okayama University Graduate School of Medicine, Dentistry, and Pharmaceutical Sciences, 2-5-1 Shikata-cho, Okayama 700-8558, Japan
[b] Department of Virology II, National Institute of Infectious Diseases, 1-23-1 Toyama, Shinjuku-ku, Tokyo 162-8640, Japan

ARTICLE INFO

Article history:
Received 16 November 2010
Received in revised form 4 February 2011
Accepted 4 February 2011
Available online 12 February 2011

Keywords:
HCV
HCV RNA replication system
RBV
IMPDH inhibitor

ABSTRACT

Ribavirin (RBV) is a potential partner of interferon (IFN)-based therapy for patients with chronic hepatitis C. However, to date, its anti-hepatitis C virus (HCV) mechanism remains ambiguous due to the marginal activity of RBV on HCV RNA replication in HuH-7-derived cells, which are currently used as the only cell culture system for robust HCV replication. We investigated the anti-HCV activity of RBV using novel cell assay systems. The recently discovered human hepatoma cell line, Li23, which enables robust HCV replication, and the recently developed Li23-derived drug assay systems (ORL8 and ORL11), in which the genome-length HCV RNA (O strain of genotype 1b) encoding renilla luciferase efficiently replicates, were used for this study. At clinically achievable concentrations, RBV unexpectedly inhibited HCV RNA replication in ORL8 and ORL11 systems, but not in OR6 (an HuH-7-derived assay system). The anti-HCV activity of RBV was almost cancelled by an inhibitor of equilibrative nucleoside transporters. The evaluation of the anti-HCV mechanisms of RBV proposed to date using ORL8 ruled out the possibility that RBV induces error catastrophe, the IFN-signaling pathway or oxidative stress. However, we found that the anti-HCV activity of RBV was efficiently cancelled with guanosine, and demonstrated that HCV RNA replication was notably suppressed in inosine monophosphate dehydrogenase (IMPDH)-knockdown cells, suggesting that the antiviral activity of RBV is mediated through the inhibition of IMPDH. In conclusion, we demonstrated for the first time that inhibition of IMPDH is a major antiviral target by which RBV at clinically achievable concentrations inhibits HCV RNA replication.

1. Introduction

Hepatitis C virus (HCV) infection causes chronic hepatitis, which often leads to liver cirrhosis and hepatocellular carcinoma (Thomas, 2000). Since approximately 170 million people are infected with HCV worldwide, HCV infection is a serious global health problem (Thomas, 2000). HCV is an enveloped positive single-stranded RNA virus of the *Flaviviridae* family. The HCV genome encodes a large polyprotein precursor of approximately 3000 amino acids, which is cleaved into in the following order: Core, envelope 1 (E1), E2, p7, non-structural protein 2 (NS2), NS3, NS4A, NS4B, NS5A, and NS5B (Kato et al., 1990).

The current standard therapy for patients with chronic hepatitis C is a combination of pegylated-interferon (PEG-IFN) and ribavirin (RBV). This treatment currently achieves a sustained virological response (SVR) greater than 50% (Chevaliez et al., 2007). However, the mechanism of RBV activity in patients with chronic hepatitis C is still ambiguous. To date, five distinct mechanisms have been proposed: (a) RBV acts as an RNA mutagen that causes mutations of the HCV RNA genome and induces a so-called "error catastrophe" (Feld and Hoofnagle, 2005); (b) RBV enhances the IFN-signaling pathway (Feld et al., 2010; Thomas et al., 2011); (c) RBV induces GTP depression by inhibiting inosine monophosphate dehydrogenase (IMPDH) (Zhou et al., 2003); (d) RBV directly inhibits NS5B-encoded RNA-dependent RNA polymerase (Feld and Hoofnagle, 2005); (e) RBV enhances host T-cell mediated immunity by switching the T-cell phenotype from type 2 to type 1 (Lau et al., 2002). Unfortunately, no groups have clarified the anti-HCV mechanism of RBV at clinically achievable concentrations (5–14 μM) (Feld et al., 2010; Pawlotsky et al., 2004; Tanabe et al.,

Abbreviations: HCV, hepatitis C virus; E1, envelope 1; NS2, nonstructural protein 2; PEG, polyethylene glycol; IFN, interferon; RBV, ribavirin; SVR, sustained virological response; IMPDH, inosine monophosphate dehydrogenase; RL, renilla luciferase; EC_{50}, 50% effective concentration; VE, vitamin E; NBMPR, *S*-(4-nitrobenzyl)-6-thioinosine; MPA, mycophenolic acid; CsA, cyclosporine A; STAT1, signal transducer and activator of transcription 1; ENT, equilibrative nucleoside transporter; RT-PCR, reverse-transcription polymerase chain reaction; ISG, IFN-stimulated gene; IRF7, IFN regulatory factor 7; IP-10, IFN-gamma-inducible protein-10; GAPDH, glyceraldehyde-3-phosphate dehydrogenase; 5′-UTR, 5′-untranslated region; Neo^R, neomycin-resistance gene; CNT, concentrative nucleoside transporter; EC_{90}, 90% effective concentration; CFE, colony-forming efficiency; MMPD, merimepodib.

* Corresponding author. Tel.: +81 86 235 7385; fax: +81 86 235 7392.
E-mail address: nkato@md.okayama-u.ac.jp (N. Kato).

0168-1702/$ – see front matter © 2011 Elsevier B.V. All rights reserved.
doi:10.1016/j.virusres.2011.02.005

2004). Although most of the above mechanisms were proposed based on studies using HuH-7 (human hepatoma cell line)-derived cells, which are currently used as the only cell culture system for robust HCV replication, the effective concentrations (50–1000 μM) of RBV were much higher than the clinically achievable concentrations (Feld and Hoofnagle, 2005; Feld et al., 2010; Lau et al., 2002; Pawlotsky et al., 2004; Thomas et al., 2011; Zhou et al., 2003). Indeed, our HuH-7-derived cell assay system (OR6) (Ikeda et al., 2005; Naka et al., 2005), in which genome-length HCV RNA (O strain of genotype 1b) encoding renilla luciferase (RL) efficiently replicates, also showed that the 50% effective concentration (EC_{50}) of RBV was approximately 100 μM (Naka et al., 2005).

Recently, we found a new human hepatoma cell line, Li23, that enables robust HCV RNA replication (Kato et al., 2009). We showed by microarray analysis that Li23 cells possessed expression profiles rather different from those in HuH-7 cells (Kato et al., 2009), and that the expression profile of Li23 cells was distinct from those of frequently used other hepatoma cell lines (Mori et al., 2010). We further developed Li23-derived cell culture assay systems (ORL8 and ORL11) in which genome-length HCV RNA (O strain of genotype 1b) encoding RL efficiently replicates (Kato et al., 2009). Here, we unexpectedly observed through the use of these cell culture assay systems the first evidence of anti-HCV activity of RBV at clinically achievable concentrations, and obtained the convincing data that the anti-HCV mechanism of RBV is mediated through the inhibition of IMPDH.

2. Materials and methods

2.1. Cell cultures

HuH-7-derived cells harboring an HCV replicon or genome-length HCV RNA were maintained with medium containing G418 (0.3 mg/ml) as described previously (Ikeda et al., 2005). Li23-derived polyclonal sORL8 and sORL11 cells harboring an HCV replicon were established by the transfection of ORN/3-5B/QR,KE,SR RNA (Kato et al., 2009) into the cured OL8 and OL11 cells, respectively. Li23-derived cells harboring an HCV replicon or genome-length HCV RNA were maintained as described previously (Kato et al., 2009). Cured cells, from which the HCV RNA had been eliminated by IFN treatment, were also maintained as described previously (Kato et al., 2009).

2.2. RL assay

RL assay was performed as described previously (Ikeda et al., 2005; Kato et al., 2009). The experiments were performed at least in triplicate.

2.3. Reagents

RBV was kindly provided by Yamasa (Chiba, Japan). Human IFN-α, vitamin E (VE), phloridzin dihydrate, *S*-(4-nitrobenzyl)-6-thioinosine (NBMPR), and mycophenolic acid (MPA) were purchased from Sigma–Aldrich (St. Louis, MO). Cyclosporine A (CsA) was purchased from Calbiochem (San Diego, CA). Guanosine and adenosine were purchased from Wako Pure Chemical Industries, Ltd. (Osaka, Japan).

2.4. Cell viability

Cell viability was examined by the method described previously (Kato et al., 2009). The experiments were performed in triplicate.

2.5. Western blot analysis

The preparation of cell lysates, sodium dodecyl sulfate–polyacrylamide gel electrophoresis and immunoblotting analysis with a PVDF membrane were performed as previously described (Kato et al., 2003). The antibodies used in this study were those against Core (CP11; Institute of Immunology, Tokyo, Japan), NS5B (a generous gift from Dr. M. Kohara, Tokyo Metropolitan Institute of Medical Science), signal transduction and activator of transcription 1 (STAT1) and phospho-STAT1 (Tyr701) (BD Transduction Laboratories, Lexington, KY) and equilibrative nucleoside transporter 1 (ENT1) (Abgent, San Diego, CA). β-actin antibody (Sigma–Aldrich) was used as the control for the amount of protein loaded per lane. Immunocomplexes were detected by using a Renaissance enhanced chemiluminescence assay (Perkin Elmer Life Sciences, Boston, MA).

2.6. Reverse transcription-polymerase chain reaction (RT-PCR)

Total RNA from the cultured cells was extracted with an RNeasy Mini Kit (Qiagen, Valencia, CA). RT-PCR was performed by a method described previously (Dansako et al., 2003) using the following primer pairs: IFN-stimulated gene (ISG) 15 (346 bp), 5′-GCCTTCCAGCAGCGTCTGGC-3′ and 5′-GCAGGCGCAGATTCATGAACACGG-3′; IFN regulatory factor 7 (IRF7) (221 bp), 5′-AGCTGCGCTACACGGAGGAACTG-3′ and 5′-CCACCAGCTCTTGGAAGAAGAC-3′; IFN-gamma-inducible protein-10 (IP-10) (111 bp), 5′-GGCCATCAAGAATTTACTGAAAGCA-3′ and 5′-TCTGTGTGGTCCATCCTTGGAA-3′; ENT1 (382 bp), 5′-GAGTTTCA-GTCTCCAACTCTCAG-3′ and 5′-GCATCGTGCTCGAAGACCACAG-3′; ENT2 (306 bp), 5′-CTTGTGTTGGTCTTCACAGTCAC-3′ and 5′-GGTGATGAAGTAGGCATCCTGTG-3′; ENT3 (350 bp), 5′-GTCTTCTTCATCACCAGCCTCATC-3′ and 5′-GTGCTGAGGTAGCCGT-TGCTGAG-3′; glyceraldehyde-3-phosphate dehydrogenase (GAPDH) (334 bp), 5′-GACTCATGACCACAGTCCATGC-3′ and 5′-GAGGAGACCACCTGGTGCTCAG-3′.

2.7. Infection of cells with secreted HCV

The inoculum was prepared from HCV-JFH1 (Wakita et al., 2005)-infected HuH-7-derived RSc cells (Ariumi et al., 2007; Kato et al., 2009) at 5 days postinfection and then stored at −80 °C after filtering through a 0.20-μm filter (Kurabo, Osaka, Japan) until use. ORL8c or RSc cells (each 5×10^4) were cultured for 24 h before infection. The cells were infected with 50 μl (equivalent to a multiplicity of infection of 0.05–0.1) of inoculum and maintained for several days until RBV treatment.

2.8. Quasispecies analysis of HCV RNA

ORL8 cells were treated with or without RBV (50 μM) for 72 h. Total RNA from the cultured cells was extracted with an RNeasy Mini Kit (Qiagen). To amplify genome-length HCV RNA, RT-PCR was performed separately in two fragments using KOD-plus DNA polymerase (Toyobo) as described previously (Ikeda et al., 2005; Kato et al., 2003). The two PCR products (the 6.0 kb region covering 5′-untranslated region (5′-UTR) to NS3 and the 6.1 kb region covering NS2 to NS5B) were subcloned into the *Xba*I site of pBR322MC, and sequence analysis of the region encoding RL to the neomycin-resistance gene (Neo^R) (1953 nts), NS5A (1341 nts), or NS5B (1773 nts) was performed as described previously (Ikeda et al., 2005). Synonymous and nonsynonymous substitutions at variance with the parental ORN/C-5B/QR,KE,SR sequences (Kato et al., 2009) were determined. To examine the error frequency of KOD-plus DNA polymerase in the PCR amplification, PCR using the plasmid containing ORN/C-5B/QR,KE,SR sequences was performed separately in the